ADAPTIVE FORMATION OF BEAMS AND IMAGES IN THE TURBULENT ATMOSPHERE

V.P. Lukin

Institute of Atmospheric Optics,
Siberian Branch of the Russian Academy of Sciences, Tomsk,
Received December 13, 1993

Investigations on adaptive optics conducted during the last fifteen years at the Institute of Atmospheric Optics, Siberian Branch of the Russian Academy of Sciences are summarized in this paper. The atmospheric turbulence is one of the most important factors which determine the limit of achievable characteristics of the present optoelectronic systems. Therefore, the main attention is paid in the paper to the adaptive optics capability to eliminate the effect of atmospheric turbulence on the formation of laser beams and optical images.

This paper is entirely based on the investigations performed by the author himself or under his supervision at the Laboratory of Applied and Adaptive Optics of the IAO, SB RAS.

The paper is written as a review, so every section's title is followed by the indication of a year when the investigations described were completed.

Investigations on correction for fluctuations in optical beams and images formed in a turbulent atmosphere, have been started at the IAO in the early 80s. Just at that time we have realized that simplest correction algorithms (e.g., the ones correcting only for the tilt of the phase front) are preferable because multicomponent adaptive correctors are too hard for control in the turbulent atmosphere.

1. CORRELATION BETWEEN RANDOM DISPLACEMENTS OF THE GRAVITY CENTERS OF A BEAM AND RELEVANT IMAGE (1978)

We start with Ref. 1 where we have examined the possibility of correcting for random angular displacements of the energy center of an optical beam propagating in the turbulent atmosphere, by controlling random angular position of an image center of some reference beam. A reference beam is obviously formed under the action of the same inhomogeneities of a turbulent atmosphere as that to be corrected (Fig. 1).
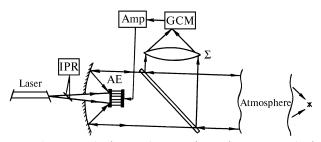

FIG. 1. An optical experiment where the same optical system forms both a beam and an image. Designations: Σ − tracking aperture, AE − adaptive element, IPR − image photorecorder, GCM − meter of image's center of gravity, and Amp − amplifier to control adaptive element.

Let us examine the cross correlation between random displacements of the center of gravity of an optical beam formed in a turbulent medium layer and the image at the focal plane of an optical system. The former ones are determined[2] by the vector

$$\rho_c = \frac{1}{P_0} \int_0^x d\xi \, (x - \xi) \int\!\!\!\int_{-\infty}^{+\infty} d^2 r \, I(\xi, \mathbf{r}) \, \nabla_r \, n_1(\xi, \mathbf{r}) , \qquad (1)$$

where $n_1(\xi, \mathbf{r})$ describes refractive index fluctuations at the point $(\xi, \mathbf{r})$, $I(\xi, \mathbf{r})$ is the field intensity at the same point (the field source is considered to be at the origin of a coordinate system in the plane $\xi = 0$), x is the depth of the turbulent layer,

$$P_0 = \int\!\!\!\int_{-\infty}^{+\infty} d^2 r \, I(0, \mathbf{r}) . \qquad (2)$$

The latter ones (when considering an equivalent thin lens with the focal length F and area $\Sigma = \pi R^2$) are expressed in the phase approximation as follows:

$$\rho_F = - \frac{F}{k \, \Sigma} \int\!\!\int d^2\rho \, \nabla_\rho \, S(x, \rho) , \qquad (3)$$

where k is the radiation wave number, and $S(x, \rho)$ describes the wave phase fluctuations at the aperture of the optical system (in the plane $\xi = x$) at the point ρ. The cross correlation between random vectors ρ_c and ρ_F is

$$K = <\rho_c \, \rho_F>/(<r_c^2><r_F^2>)^{1/2} , \qquad (4)$$

where angular brackets mean averaging over ensemble of random function $n_1(\xi, \mathbf{r})$ values. Different optical cases (i.e., correction using auxiliary source, when the corrected and the reference beams are counter directed, and the one using radiation reflected from the mirror or an object) from the viewpoint of correlation K calculation differ only in analytical expressions for $S(x, \rho)$. We use for phase fluctuations the approximation of smooth perturbation method[2] and assume the corrected beam to be Gaussian with the parameters a and f. When averaging Eq. (4) over the refractive index fluctuations we make

use of the fact that no correlation exists between local and integral random variables.[2] Further we use

$$<d^2n(\kappa_1, \xi_1)\, d^2n(\kappa_2, \xi_2)> =$$

$$= 2\pi\delta\,(\kappa_1 + \kappa_2)\,\delta\,(\xi_1 - \xi_2)\,\Phi_n(\kappa_1, \xi_1)\,d^2\kappa_1\,d^2\kappa_2\,,$$

where

$$n_1(\mathbf{r}) = \int\limits_{-\infty}^{+\infty}\!\!\int \mathrm{d}^2n\,(\kappa, \xi)\,\exp\,(i\,\kappa\,\rho)\,,$$

$\Phi_n(\kappa_1, \xi_1)$ is spectral density of the refractive index fluctuations. To simplify calculations, we replace physical aperture of the optical system by Gaussian one

$$\int\limits_{\Sigma}\!\!\int \mathrm{d}^2\rho \Rightarrow \int\limits_{-\infty}^{+\infty}\!\!\int \mathrm{d}^2\rho\,\exp\,(-\,\rho^2/2\,R_0^2)\,.$$

We also assume that average intensity $<I(\xi, \mathbf{r})>$ and spectrum $\Phi_n(\kappa, \xi)$ are isotropic and use the average intensity in the form

$$<I(\xi, \rho)> = \frac{a^2}{a_{\mathrm{eff}}^2(x)}\,\exp\,[-\,r^2\,/\,a_{\mathrm{eff}}^2(\xi)]\,, \tag{5}$$

where beam's effective size is

$$a_{\mathrm{eff}}^2(\xi) = a^2\left[(1-\xi\,/\,f)^2 + \Omega^{-2} + \Omega^{-2}\left(\tfrac{1}{2}\,D_s\,(2\,a)\right)^{6/5}\right]\,,$$

$\Omega = ka^2/\xi$, and $D_s(2a)$ is the structure function of phase.

Integrals in Eq. (4) will be calculated using the spectrum

$$\Phi_n(\kappa, \xi) = 0.033\,C_n^2(\xi)\,\kappa^{-11/3}\,\{1 - \exp\,(-\,\kappa^2/k_0^2)\}\,, \tag{6}$$

which allows for deviation from the power law in the region of outer turbulence scale κ_0^{-1}. Consider the most interesting case of large receiving apertures $(kR_0^2 \gg x)$. For the path with homogeneous turbulence $(C_n^2(\xi) = C_n^2)$ computed values of K are presented in Table I. We have also computed correlations for the case when reflected radiation is used.[1]

Consider the control algorithm for correcting for the beam's random displacements by measuring displacements of its image. It can be taken in the form of the signal

$$\alpha\!\left(\frac{x}{F}\right)\,(a^2/2\,R_0^2)^{-1/6}\,\rho_{\mathrm{F}}\,,$$

where α is a feedback coefficient chosen so that the functional

$$\min_{\alpha}\,<\!\left(\rho_c - \alpha\!\left(\frac{x}{F}\right)(a^2/2R_0^2)^{-1/6}\rho_F\right)^2\!>^2 \tag{7}$$

is minimum. It also includes the sign of correlation $<\rho_c\,\rho_F>$. The value of functional (7) describes residual distortion. As Table I shows, the variance of permanent

distortions caused by beam's random displacement comes to only 15—25% of the one without a correction.

Since any actuator in a feedback loop (including the adaptive system correcting for the tilt of the phase front) has some time constant τ, the value of correlation K differs from the one computed by Eq. (4), and in the general case it is a function of τ

$$K(\tau) = <\rho_c(\tau)\,\rho_F(0)>/[<\rho_c^2>\,<\rho_F^2>]^{1/2}\,. \tag{8}$$

It can be shown that the maximum value of $|K|$ is reached when $2R_0^2 = a^2$. There we have

$$K(\tau) = -\,0.87\,\,_1F_1^{1/2}\left(\frac{1}{6},1;v^2\tau^2/2a^2\right)\,. \tag{9}$$

As seen from Eq. (9), an essentially high correction efficiency can be reached if $\tau < a/v$, where a is the initial size of the beam and v is the average wind velocity.

It should be noted that this way of correction is most efficient up to distances where the condition

$$a < (1.45\,k^2\,C_n^2\,x)^{-3/5}$$

is fulfilled.

The reduction of the average beam size in the plane of observation occurring due to such a correction causes relative increase in the incident field intensity. In some cases this simplest correction algorithm can be successfully used instead of the full phase correction (e.g., in the systems which need to minimize the beam's random fluctuations as a whole to random low—frequency refraction)

2. COMPARATIVE CHARACTERISTICS OF THE CORRECTION ALGORITHMS (1980)

An essential step of our investigations into this problem was the study of comparative characteristics of two correction algorithms, namely, wave front conversion (WFC) and phase conjugation (PC). In Ref. 3 the case of using a point reference source in the receiving plane is described.

Let the propagation of optical radiation be given by the equation

$$\begin{cases} 2ik\,\dfrac{\partial}{\partial\,x}\,U(x, \rho) + C_{\mathrm{r}}^2\,U + k^2\,\varepsilon_1(x, \rho)\,U = 0\,, \\ U(x_0, \rho) = U_0(\rho)\,, \end{cases} \tag{10}$$

and the turbulent medium be confined between the transmission plane $x = x_0$ and the receiving one $x = x_1$. The field in the receiving plane may be presented as the expansion

$$U(x_1, \rho) = \int\!\!\int \mathrm{d}^2\rho_1\,U_0(\rho_1)\,G(x_1, \rho;\,x_0, \rho_1)\,, \tag{11}$$

where G is Green's function for the equation conjugated with Eq. (10).

Let us consider residual distortions of optical radiation in the receiving plane with the correction based on "measurement" of field fluctuations of the reference source (beacon) placed in the plane $x = x_1$ at a point $\rho = \rho_b$. The WFC algorithm introduces predistortion into the initial field

V.P. Lukin

154 Atmos. Oceanic Opt. /бфкрт 1995/ Vol. 8, No. 3

TABLE I.

	$\Omega \gg 1,\ \Omega^{-2}\left(\frac{1}{2}D_s(2a)\right)^{6/5} \ll 1$		$\Omega = 1$		$\Omega \ll 1$
	$x/f = 0$	$x/f = +1$	$x/f = 0$	$x/f = +1$	$R_0 \gg a,\ R_0^2 \gg a^2\,\Omega^{-2}\left[1+\left(\frac{1}{2}D_s(2a)\right)\right]^{6/5}$
$R_0 \gg a$	$K = -0.87\left(\frac{2\,R_0^2}{a^2}\right)^{-1/12}$	$K \simeq -0.82\left(\frac{2\,R_0^2}{a^2}\right)^{-1/12}$	$K \simeq -0.87\left(\frac{2\,R_0^2}{a^2}\right)^{-1/12}$	$K \simeq -0.84\left(\frac{2\,R_0^2}{a^2}\right)^{-1/12}$	
$2\,R_0^2 = a^2$	$K = -0.87$	$K \simeq -0.82$	$D_s(2\,a) \ll 1$: $K \simeq -0.81$ — $D_s(2\,a) = 1\dots2$: $K \simeq -0.70$	$D_s(2\,a) \ll 1$: $K \simeq -0.78$ — $D_s(2\,a) = 1\dots2$: $K \simeq -0.67$	$K \simeq 0.61\,\Omega^{-1/6}\left(\frac{2\,R_0^2}{a^2}\right)^{-1/12}$
			$D_s(2\,a) \gg 1$: $K \simeq -1.4\,D_s^{-1/5}(2\,a)$	$K \simeq -1.34\,D_s^{-1/5}(2\,a)$	$R_0 \gg a,\ R_0^2 \ll a^2\,\Omega^{-2}\left[1+\left(\frac{1}{2}D_s(2a)\right)\right]^{6/5}$
$R_0 \ll a$	$K = -0.7\left(\frac{a^2}{2\,R_0^2}\right)^{-1/12}\Omega^{-1/6}$	$K \simeq -0.62\left(\frac{a^2}{2\,R_0^2}\right)^{-1/12}\Omega^{-1/6}$	$D_s(2\,a) \ll 1$: $K \simeq -0.87\left(\frac{a^2}{2\,R_0^2}\right)^{-1/12}$ — $D_s(2\,a) = 1\dots2$: $K \simeq -0.81\left(\frac{a^2}{2\,R_0^2}\right)^{-1/12}$ — $D_s(2\,a) > 1$: $K \simeq -1.26\left(\frac{a^2}{2\,R_0^2}\right)^{-1/12}\times\left(\frac{1}{2}D_s(2a)\right)^{-1/5}$	$D_s(2\,a) \ll 1$: $K \simeq -0.84\left(\frac{a^2}{2\,R_0^2}\right)^{-1/12}$ — $D_s(2\,a) = 1\dots2$: $K \simeq -0.78\left(\frac{a^2}{2\,R_0^2}\right)^{-1/12}$ — $D_s(2\,a) > 1$: $K \simeq -1.17\left(\frac{a^2}{2\,R_0^2}\right)^{-1/12}\times\left(\frac{1}{2}D_s(2a)\right)^{-1/5}$	$K \simeq -0.85\,\Omega^{-1/6}\left(\frac{a^2}{2\,R_0^2}\right)^{-1/12}\left(\frac{1}{2}D_s(2a)\right)^{-1/5}$

$$U_0(\rho)_c = U_0(\rho)\, G^*(x_1, \rho_b;\, x_0, \rho)\, . \qquad (12)$$

using the field of a reference source. As a result of this correction, one can provide focusing of a plane wave $(U_0(\rho) = 1)$ at the beacon point

$$U(x_1, \rho)_c = \int\!\!\int d^2\rho_1 G(x_1, \rho;\, x_0, \rho_1) G^*(x_1, \rho_b;\, x_0, \rho_1) = \delta(\rho_b).$$

Therefore, the WFC algorithm corrects the field (11) to the reference wave.

However, the use of the WFC algorithm in some cases faces certain difficulties. Adaptive systems operating according to the PC algorithm find more wide application when forming optical radiation propagating through the turbulent atmosphere.

The PC algorithm suggests correction of the optical wave distortions caused by random medium inhomogeneities. It is used to provide an optical system with the diffraction limited performances. To estimate the quality of this correction, let us examine the behavior of distribution moments of the intensity of the corrected field.

The PC algorithms introduce the predistortions into the initial distribution of the field which in contrast to Eq. (12) allow only for the reference spherical wave phase fluctuations

$$U_0(\rho)_c = U_0(\rho)\, G^*(x_1, \rho_b;\, x, \rho)/G_0^*(x_1, \rho_b;\, x, \rho)\, , \qquad (13)$$

where G_0^* satisfies homogeneous $(\varepsilon_1 = 0)$ equation (10). Let us compute distribution of average intensity and variance of the intensity fluctuations of the corrected field. The initial field is assumed to be a Gaussian beam

$$U_0(\rho) = \exp(-\,\rho^2\,/\,2\,a^2).$$

The distribution of the average intensity of the field corrected according to the PC algorithm is given as follows[3]

$$\langle I(x_1, \rho)\rangle_c = \left(\frac{k}{2p(x_1 - x_0)}\right)^2 \int\!\!\int d^4\rho_{1,2}\, U_0(\rho_1)\, U_0^*(\rho_2) \times$$

$$\times \exp\Bigg\{ i\,k\,\frac{(\rho_1^2 - \rho_2^2)}{2(x_1 - x_0)} - i\,k\,(\rho - \rho_b)\frac{(\mathbf{r}_1 - \mathbf{r}_2)}{(x_1 - x_0)} -$$

$$-\,D_s(x_1, \rho - \rho_b;\, x_0, 0) - D_s(x_1, 0;\, x_0, \rho_1 - \rho_2) +$$

$$+\frac{1}{2}D_s(x_1, \rho_b - \rho;\, x_0, \rho_1 - \rho_2) + \frac{1}{2}\,D_s(x_1,\, \rho - \rho_b;\, x_0,\, \rho_1 - \rho_2)\Bigg\}, \quad (14)$$

where for power Kolmogorov spectrum of the refractive index fluctuations the structural function takes the form

$$D_s(x_1, \rho;\, x_0, \rho_1) = 2.91 k^2 C_n^2 \int_{x_0}^{x_1} d\xi \left|\frac{(\xi - x_0)}{(x_1 - x_0)}\rho + \frac{(x_1 - \xi)}{(x_1 - x_0)}\rho_1\right|^{5/3} \quad (15)$$

(C_n^2 is the structural parameter of the refractive index).

The vacuum intensity distribution within the beam is

$$I_0(\mathbf{r}) = \frac{\Omega^2}{1 + \Omega^2}\exp\!\left(-\frac{\Omega\,q\,r^2}{1 + \Omega^2}\right),$$

where $q = \kappa r_0^2/(x_1 - x_0)$, $\Omega = \kappa a^2/(x_1 - x_0)$, $\rho = \mathbf{r}\,r_0$, and $r_0 \approx (1.45\kappa^2 C_n^2(x_1 - x_0))^{-3/5}$ is field's coherence length.

In the case of wide optical beams $(\Omega > 1)$, we have from Eq. (14)

$$\langle I(x_1, \mathbf{r})\rangle_c \approx q\,\Omega\,\frac{\exp\left(-\,q\,v^2/\,[q/\Omega(1 + \Omega^2) + 4\,\gamma]\right)}{q/\Omega(1 + \Omega^2) + 4\,\gamma}\,, \qquad (16)$$

where $\gamma \approx 1$. Therefore, the distribution of average intensity after correction practically coincides with the vacuum one while $q\Omega \gg 1$, this condition for sufficiently wide beams $(\Omega \gg 1)$ can be satisfied even for "strong" fluctuations $(q < 1)$.

Consider now the intensity fluctuations of a corrected field. The value of variance σ_c^2 can be taken as the intensity standard for residual fluctuations. For "weak" fluctuations $(q \gg 1,\ q > \Omega)$ $\sigma_c^2 \sim (q/\Omega)^2 \ll 1$, i.e., fluctuations are fully suppressed. As fluctuations increase, i.e., when $q\Omega > 1$ but $q < \Omega$, $\sigma_c^2 \sim 0.13\,(q/\Omega)^{1/6}\,r^2$. Finally, for "strong" fluctuations when $q\Omega < 1$, no correction is practically performed.

In conclusion of this section it may be said that PC algorithm using the point reference source is rather efficient: it reproduces quite well the distribution of average intensity and essentially suppresses intensity fluctuations in the transmitted radiation. In narrow beams applications the PC algorithm can use plane wave or a wide beam as a reference wave.

3. CORRECTION FOR RANDOM ANGULAR DISPLACEMENTS OF OPTICAL BEAMS (1981)

This section is devoted to correction[4] for random tilts of the wave front of a wide $(\Omega \gg 1)$ optical beam. As a result of application of the PC algorithm we get for corrected field in the x_1 plane

$$U_c(x_1, \rho) = \int\!\!\int d^2\rho_1 U_0(\rho_1) G(x_1, \rho;\, x_0, \rho_1)\exp(-\,i\,\alpha\,\rho_1), \quad (17)$$

where G is Green's function and α is the vector characterizing the random tilt of the phase front of a reference spherical wave in the x_0 plane within the limits of transmitting aperture. The tilt correction is introduced in the form of predistortions of the initial distribution $U_0(\rho)$ in the x_0 plane.

Efficiency of the correction (17) apparently depends on the algorithm of determining the vector α. This can be done using series expansion of the reference phase over Zernike polynomials but this way is rather complicated. More simple algorithm for determining α is provided by measuring the vector of displacements of the gravity center of the reference source image formed by a lens with the focal length F and aperture $W(\rho)$:

$$\rho_F = -\frac{F}{\kappa}\,\frac{\int\!\!\int d^2\rho\,\nabla\,S(\rho)\,W(\rho)}{\int\!\!\int d^2\rho\,W(\rho)}\,. \qquad (18)$$

Being related to the focal length, ρ_F gives a quantitative characteristic of the phase front rotation.

For further calculations we rewrite[4] the coherence function of the corrected field (17) in the form

$$\Gamma_c(x_1, \rho_1, \rho_2) = \int\!\!\int d^4 r_{1,2}\, U_0(\mathbf{r}_1)\, U_0^*(\mathbf{r}_2) \times$$

$$\times \langle G(x_1, \rho_1;\, x_0, \mathbf{r}_1)\, G^*(x_1, \rho_2;\, x_0, \mathbf{r}_2)\exp(-i\alpha(\mathbf{r}_1 - \mathbf{r}_2))\rangle. \quad (19)$$

In calculations we use phase approximation[2] for the Green's function

$$\langle G(x_1, \rho_1; x_0, \mathbf{r}_1)\, G^*(x_1, \rho_2; x_0, \mathbf{r}_2)\, \exp\left(- i\, \alpha\, (\mathbf{r}_1 - \mathbf{r}_2)\right)\rangle =$$

$$= G_0(x_1, \rho_1; x_0, \mathbf{r}_1) G_0^*(x_1, \rho_2; x_0, \mathbf{r}_2)\, \langle \exp\{i\, [S(x_1, \rho_1; x_0, \mathbf{r}_1) -$$

$$- S(x_1, \rho_2; x_0, \mathbf{r}_2)] - i\, \alpha\, (\mathbf{r}_1 - \mathbf{r}_2)\}\rangle ,$$

where

$$G_0(x_1, \rho_1; x_0, \mathbf{r}_1) = \frac{\kappa}{2\pi i\, |x_1 - x_0|}\, \exp\left\{ ik\, \frac{(\rho_1 - \rho_1)^2}{2\, |x_1 - x_0|}\right\}$$

is Green's function for empty space. For a Gaussian random field $S(x_1, \rho_1; x_0, \mathbf{r}_1)$ we have

$$\langle \exp\{i\, [S(x_1, \rho_1; x_0, \mathbf{r}_1) - S(x_1, \rho_2; x_0, \mathbf{r}_2)] - i\, \alpha\, (\mathbf{r}_1 - \mathbf{r}_2)\}\rangle =$$

$$= \exp\left\{ -\frac{1}{2}\, D_s(x_1, \rho_1 - \rho_2; x_0, \mathbf{r}_1 - \mathbf{r}_2) + \frac{1}{2}\, \langle\alpha^2\rangle\, (\mathbf{r}_1 - \mathbf{r}_2)^2 + \right.$$

$$+ (\mathbf{r}_1 - \mathbf{r}_2)\, \langle\alpha\, ([S(x_1, \rho_2; x_0, \mathbf{r}_2) - \alpha\, \mathbf{r}_2] - $$

$$\left. - [S(x_1, \rho_1; x_0, \mathbf{r}_1) - \mathbf{a}\, \mathbf{r}_1])\rangle\right\}. \tag{20}$$

In earlier calculations[5] of the average value in Eq. (19) it was assumed that no correlation between random tilts of the whole wave front α (within aperture limits) and high–frequency phase fluctuations $S(\mathbf{r}) - \alpha\mathbf{r}$ occurs. Based on Fried's approximation, we obtained for a Gaussian beam

$$U_0(\mathbf{r}) = \exp\left[- r^2\, (1/2\, a^2 + i\, k/z\, f)\right]$$

the following expression:

$$\langle I_c(x_1, \mathbf{r})\rangle = \frac{q\Omega}{4\pi} \int\int \mathrm{d}^2\rho\, \exp\left\{ -\frac{q}{4\,\pi}\left(1 + \frac{\Omega^2\,(q - q_F)^2}{q^2}\right) \times \right.$$

$$\times\, \rho^2 + i\, q\, \mathbf{r}\, \rho - 0.54\, k^2\, C_n^2\, (x_1 - x_0)\, r^{5/3}\, \rho^{5/3} +$$

$$\left. + 0.34\, k^2\, C_n^2\, (x_1 - x_0)\, a_0^{-1/3}\, r_0^2\, \rho^2\right\}, \tag{21}$$

where $\Omega = ka^2/(x_1 - x_0)$, $q_F = kr_0^2/F$. Here a_0 is the aperture size of a device that measures random tilt of the wave front α according to algorithm (18). It can be shown from Eq. (21) that a proper choice of a_0 makes the distribution $\langle I_c(x_1, \mathbf{r})\rangle$ close to the vacuum one. The optimum value of a_0 is about $2\, r_0$. This adaptive correction is efficient when $q\Omega \gg 1$.

For experimental verification of these results[4] we used the optical arrangement presented in Fig. 2. The measurer 5 was an optoelectronic device measuring the gravity center displacements of the reference beam image. The signal from it passed to a ceramic deflector 6 changing the direction of beam propagation. We used collimated ($a = 1$ cm) laser beam, the atmospheric propagation distance was 130 m 1.5 m above surface. The distribution of average beam intensity was recorded on a film. Figure 3 shows distribution cross sections of the average beam intensity with (1) and without (2) correction. Increase of axial intensity in the corrected case is manifest.
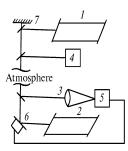

FIG. 2. Block diagram of the optical device: 1 and 2 – laser sources of reference and initial beams, 3 – lens, 4 – photorecorder, 5 – measurer of fluctuations of incidence angles, 6 – optical beam deflector, and 7 – mirror reflector.
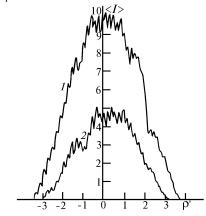

FIG. 3. Comparison of the distributions of average intensity of corrected (1) field and of the field without any correction (2).

Correction mechanism may be modified by using reflected radiation as a reference one. For this purpose we have used a plane mirror 7.

Let us now discuss again correlation between high–frequency phase fluctuations and the tilt of the wave front. As a result of correction for tilts the wave phase can be written as

$$S(\mathbf{r}) - \alpha\, \mathbf{r}.$$

Its structure function can be expressed in terms of its components as follows:

$$D_c(\mathbf{r}_1, \mathbf{r}_2) = \langle([S(\mathbf{r}_1) - \alpha\, \mathbf{r}_1] - [S(\mathbf{r}_2) - \alpha\, \mathbf{r}_2])^2\rangle = D_s(\mathbf{r}_1, \mathbf{r}_2) -$$

$$- \frac{1}{2}\, \langle\alpha^2\rangle\, (\mathbf{r}_1 - \mathbf{r}_2)^2 - 2(\mathbf{r}_1 - \mathbf{r}_2)\, \langle\alpha\, [S(\mathbf{r}_1) - S(\mathbf{r}_2)]\rangle, \tag{22}$$

where angular brackets mean averaging over an ensemble of random function values. If $\kappa_m a_0 \gg 1$, we have for Kolmogorov turbulence

$$D_s(\mathbf{r}_1, \mathbf{r}_2) \approx 1.09 k^2\, C_n^2\, (x_1 - x_0)\, |\mathbf{r}_1 - \mathbf{r}_2|^{5/3} - 0.68\, k^2 \times$$

$$\times\, C_n^2\, (x_1 - x_0)\, a_0^{-1/3}\, |\mathbf{r}_1 - \mathbf{r}_2|^2 + 1.53\, k^2\, C_n^2\, (x_1 - x_0)\, a_0^{-1/3} \times$$

$$\times\, \left\{ {}_1F_1\left(\frac{1}{6},\, 2;\, -\frac{r_1^2}{2\, a_0^2}\right) r_1\, (r_1 - r_2\, \cos\,(\mathbf{r}_1, \mathbf{r}_2)) + \right.$$

$$+ \, _1F_1 \left(\frac{1}{6}, \, 2; \, - \frac{r_2^2}{2 \, a_0^2} \right) r_2 \, (r_2 - r_1 \cos \, (\mathbf{r}_1, \, \mathbf{r}_2)) \right\} \, . \qquad (23)$$

Main peculiarity of $D_s(\mathbf{r}_1, \, \mathbf{r}_2)$ in contrast to Eq. (21) is its positive definiteness for any $\mathbf{r}_1$ and $\mathbf{r}_2$, which provides physically correct results for any relation between a and r_0. Analysis of the average intensity distribution[4] accounting for correlation between the tilts and high–frequency phase fluctuations shows that for $a \gg r_0$

$$\langle I_c(x_1, \, \mathbf{r}) \rangle \approx \langle I(x_1, \, \mathbf{r}) \rangle \, ,$$

i.e., correction only for random wave front tilts does not lead to an increase in the average intensity.

4. RECIPROCITY PRINCIPLE AND ADAPTIVE CONTROL OF OPTICAL RADIATION PARAMETERS (1982)

In this section we propose some simple applications of the adaptive control of beam parameters, based on the reciprocity principle for propagation of radiation in an inhomogeneous medium. Information about inhomogeneities distribution along the propagation path is derived from the intensity distribution in the plane of the object image.[6]

The field of an optical beam at the point $(L, \, \mathbf{R})$ of an inhomogeneous medium can be written in the form

$$U_b(L, \, \mathbf{R}) = \int \int d^2\rho \, U_0(\rho) \, G(L, \, \mathbf{R}; \, 0, \, \rho) \, , \qquad (24)$$

where $G(...)$ is Green's function or the spherical wave field. Let the point object be placed at that point $(L, \, \mathbf{R})$, whereas optical system is placed in the plane $x = 0$. The field of radiation coming from this object to the plane $x = -l$ is

$$U_S(-l, \mathbf{r}) = \int \int d^2\rho \, G(L, \mathbf{R}; 0, \rho) A(\rho) \exp(iS(\rho)) G_0(0, \rho; -l, \mathbf{r}). \qquad (25)$$

Here $A(\rho)$ is the amplitude transmittance of an optical receiver, $S(\rho)$ is the phase shift introduced by the optical system, and G_0 is Green's function for a homogeneous medium. Owing to the reciprocity principle[6,7] we have

$$G(x_0, \, \rho_0; \, x, \, \rho) = G(x, \, \rho; \, x_0, \, \rho_0) \, .$$

It is seen from Eqs. (24) and (25) that for

$$U_0(\rho) = \frac{k}{2\pi \, i \, l} A(\rho) \exp \, (i \, S(\rho)) \exp \left(i \, \frac{k \, r^2}{2 \, l} - i \, k \, \frac{\mathbf{r} \, \mathbf{r}}{l} \right) \qquad (26)$$

the field of a coherent light beam at the point $(L, \, \mathbf{R})$ coincides with that of radiation from a point source at the point $(-l, \, \mathbf{r})$ accurate to a constant factor

$$U_b(L, \, \mathbf{R}) = l \, U_S(-l, \, \mathbf{r}) \, . \qquad (27)$$

This relation is an exact corollary of the reciprocity principle and it assumes that the field of radiation from a point source placed at the point $(L, \, \mathbf{R})$ of an inhomogeneous medium, passed through a window with the transmittance $A(\rho)\exp(iS(\rho))$ and observed at the point $(-l, \, \mathbf{r})$, coincides with the field of radiation from the same source but placed at the point $(-l, \, \mathbf{r})$, passed along this path back and observed at the point $(L, \, \mathbf{R})$.

Below we consider some applications of this principle to control beam parameters in order to maximize the radiation intensity at some remote point.[6]

Choice of a proper moment for delivering a radiation pulse

To solve this problem we must record intensity distribution of radiation from a point beacon at the point $(-l, \, \mathbf{r})$ beyond the optical system with the transmittance $A(\rho)\exp(iS(\rho))$ determined from Eq. (26), and to deliver the laser pulse through the same optical system at the moment when the beacon radiation intensity is spiking. Obviously the pulse travel time must not exceed the delay time of the amplitude–phase distribution. Besides, if a collimated beam is used, observation must be done in the focal plane of optical system, whereas for a focused beam it must be done in the plane of an object image.

Aiming of a beam axis at a point object

A correct aiming of a beam axis should bring $I_b(L, \, \mathbf{R}) = U_b U_b^*$ to a maximum. Change of direction is equivalent to introduction of a phase shift to the initial field distribution, that is,

$$U_0(\rho) = U_0 \exp \, (i \, k \, \gamma \, \rho),$$

where γ is the vector of the beam axis tilt. Given the distance between the observation and the receiving aperture planes $(-l)$, we choose the transmittance so that

$$A(\rho) \exp \, (i \, S(\rho)) = C \, U_0 \exp \, (i \, k \, \rho^2/2 \, l). \qquad (28)$$

Under conditions (28) equation (26) is fulfilled when $\gamma = -\mathbf{r}/l$. Consequently, the best directions for maximizing intensity at an object will correspond to vectors $\mathbf{r}$ along which the intensity of radiation coming from an object is maximum. Therefore, when aiming a continuous radiation at an object, the beam's axis must be directed to the brightest point of the intensity distribution. This method automatically tracks the object motion.

Aiming and focusing of a beam of coherent radiation

In this case we have to make the best choice of the beam's axis tilt and focal length based on the intensity distribution in some region beyond the optical system. The initial field distribution is of the form

$$U_0(\rho) = U_0 \exp \, (i \, k \, \gamma \, \rho - i \, k \, \rho^2/2 \, F) \, , \qquad (29)$$

where the axis tilt vector γ and beam's focal length F are to be controlled. The condition (26) should be fulfilled if

$$\gamma = - \, \mathbf{r}/l \, , \quad 1/F = 1/f - 1/l \qquad (30)$$

which in turn gives $I_b(L, \, \mathbf{R}) \sim l^2 I_s(-l, \, \mathbf{r})$, i.e., intensity of radiation from a point source at the point $(-l, \, \mathbf{r})$ beyond the optical system is proportional to the intensity of the beam whose axis tilt vector γ and focal length F are determined from Eq. (30).

Therefore, the best beam's focal length F and the axis tilt vector γ, that is, the point $(-l, \, \mathbf{r})$ where the value of $l^2I(-l, \, \mathbf{r})$ is brought at maximum, are determined from Eq. (30).

It is known that in the process of an object detection, the intensity of reflected signal fluctuates as squared intensity at an object, and consequently the maximum of received signal brings also the maximum to the intensity at the object. That is why all the above mentioned methods of controlling the beam parameters can be performed with the use of reflected radiation.[6]

5. QUASIMODE CORRECTION OF AN IMAGE PASSED THROUGH THE RANDOMLY INHOMOGENEOUS MEDIUM (1982)

This section[8] is devoted to comparison of field characteristics obtained using mode correction (with correction of two dominant modes) or by correction based on analysis of distribution moments of the intensity in the image plane. It can be applied to either aiming of an optical beam through the atmosphere with the use of a reference source or improving quality of an image of a star built up with a telescope.

Let the optical wave with distorted front be incident on the telescope aperture with radius R_a. To provide the telescope with the diffraction−limited performances one should complete the measured wave front to a plane one. We consider here the phase−conjugated mode correction algorithm restricting ourselves to Y and Z axes correction of random tilts of the phase front. As a result of such a correction, the wave phase at the telescope aperture takes the form

$$\Phi_c(\mathbf{r}) = \Phi(\mathbf{r}) - \sum_{j=2}^{3} a_j\, F_j\left(\mathbf{r}/R_a\right), \tag{31}$$

where $F_2(\mathbf{r}/R_a) = 2y/R_a$ and $F_3(\mathbf{r}/R_a) = 2z/R_a$ are dominant Zernike modes, and

$$a_j = \frac{1}{R_a^2} \int\!\!\int_{-\infty}^{+\infty} d^2r\, \Phi(\mathbf{r})\, F_j\left(\mathbf{r}/R_a\right) W\left(\mathbf{r}/R_a\right).$$

Then the distribution of average intensity in the telescope focal plane ($x = f$) is as follows:

$$\langle I_f(\rho)\rangle = \frac{k^2}{4\pi^2 f^2} \int\!\!\int d^4\rho_{1,2}\, W(\rho_1/R_a)\, W(\rho_2/R_a) \times$$

$$\times \exp\left\{- i\,k\,\rho\,\frac{(\rho_1 - \rho_2)}{f}\right\} \langle\exp\{i\,[\Phi(\rho_1) - \Phi(\rho_2)] -$$

$$- i \sum_{j=2}^{3} a_j\, [F_j(\rho_1/R_a) - F_j(\rho_2/R_a)]\}\rangle. \tag{32}$$

For a random Gaussian field $\Phi(\rho)$ the averaging in the right−hand side of Eq. (32) results in

$$\langle \cdots \rangle = \exp\left\{-\frac{1}{2} D_\Phi(\rho_1 - \rho_2) + 2\frac{\langle a_2^2\rangle}{R_a^2}(\rho_1 - \rho_2)^2 + \langle a_2 a_8\rangle \times \right.$$

$$\left.\times \left[\frac{6\sqrt{8}}{R_a^4}(\rho_1^4 + \rho_2^4) - \rho_1\rho_2(\rho_1^2 + \rho_2^2) - \frac{4\sqrt{8}}{R_a^2}(\rho_1 - \rho_2)^2\right]\right\}, \tag{33}$$

where, for Kolmogorov turbulence,

$$D_\Phi(\rho_1 - \rho_2) = 6.88\,(\,|\rho_1 - \rho_2|\,/r_0)^{5/3},$$

$$\langle a_2^2\rangle = \langle a_3^2\rangle = 1.42\,(R_a/r_0)^{5/3},$$

$$\langle a_2 a_8\rangle = \langle a_3 a_7\rangle = -\,0.045\,(R_a/r_0)^{5/3},$$

(r_0 is the radius of coherence).

Recently[5] the optical transfer function $\langle\tau(\rho)\rangle$ of a telescope looking through the atmosphere was analyzed in the case of no correlation between corrected tilts and high−frequency phase fluctuations. In our designations ($\langle a_2 a_8\rangle = 0$) it corresponds to

$$\langle\tau(\rho)\rangle = K_0(\rho)\exp\left\{-3.44\,(\rho/r_0)^{5/3} + 2.86\,R_a^{-1/3}\rho^2\, r_0^{-5/3}\right\}, \tag{34}$$

where $K_0(\rho)$ is the optical transfer function of the telescope in vacuum. It is known that the expression (34) gives physically correct results but only for weak turbulence ($r_0 > R_a/2$).

The optical transfer function can be written using Eq. (33) with regard for the correlation $\langle a_2 a_8\rangle$. Thus, for Gaussian effective aperture of the telescope $W(\rho) = \exp(-\rho^2/2R_a^2)$ we obtain

$$\langle\tau(\rho)\rangle = \left[1 + 2.41\,\frac{r^2}{R_a^{1/3}\, r_0^{5/3}}\right]^{-1} \exp\left\{-3.44\,(\rho/r_0)^{5/3} + \right.$$

$$\left. +\, 3.35\,\rho^2\, R_a^{-1/3}\, r_0^{-5/3} - 0.24\,\rho^4\, R_a^{-7/3}\, r_0^{-5/3}\right\}. \tag{35}$$

Of course, the account for a greater number of expansion modes in Eq. (31) when making correction makes an optical system closer to a diffraction limited one. Nevertheless, mode correction requires the phase $\Phi(\rho)$ to be measured over the entire aperture.

To simplify this procedure we restrict ourselves when making the lowest order correction to analysis of distribution of moments of the intensity in the plane of image of an auxiliary aperture Σ (Fig. 1). In particular, the first moment determines the position of the center of gravity of image and specifies angle of the wave front arrival. Using the relation[7]

$$\alpha = -\frac{1}{k\,\Sigma} \int\!\!\int_\Sigma d^2\rho\,\nabla_\rho\,\Phi(\rho), \tag{36}$$

we obtain for the corrected phase the following expression

$$\Phi_c(\rho) = \Phi(\rho) + \alpha\,\rho\,k.$$

In Ref. 8 we have obtained an expression for the average intensity distribution of an image formed in a turbulent atmosphere

$$\langle I_f(\rho)\rangle = \frac{k^2}{4\pi^2 f^2} \int\!\!\int d^4\rho_{1,2}\, W(\rho_1/R_a)\, W(\rho_2/R_a) \times$$

$$\times \exp\left\{- i\,k\,\rho\,\frac{(\rho_1 - \rho_2)}{f}\right\} \exp\left\{-3.44\,|\rho_1 - \rho_2|^{5/3}\, r_0^{-5/3} + \right.$$

$$+\, 2.66\,|\rho_1 - \rho_2|^2\, R^{-1/3}\, r_0^{-5/3} - 5.73\,R^{-1/3}\, r_0^{-5/3} \times$$

$$\left.\times \left[\frac{\rho_1(\rho_1 - \rho_2)}{(\rho_1/R + 1)^{1/3}} - \frac{\rho_2(\rho_1 - \rho_2)}{(\rho_2/R + 1)^{1/3}}\right]\right\}. \tag{37}$$

Analysis of this result shows that a proper choice of the tracking aperture R made using such a "quasimode" correction provides the residual distortions to be of the same value as in the case of correction of only two dominating modes. Optimum value of the aperture R depends on the telescope aperture R_a and on r_0.

This algorithm can be developed by determining the instant focus of a received phase front and provides that

compensation for defocusing is done. The instant focus can be determined by evaluating higher order moments of image intensity distribution.

Correction algorithm described above is rather simple and can be recommended to improve the quality of an image constructed by telescope.

In the same paper[8] we have presented evaluations of a required frequency band of a wave front sensor to provide adaptive mode correction.

6. ADAPTIVE IMAGE CORRECTION USING A POINT REFERENCE SOURCE (1982)

Here we investigate how to improve image of an extended object formed with a coherent light through the atmospheric layer, with the use of an adaptive correction.[9] To do this, a phase conjugation algorithm corrections is used whereas information on the distribution of turbulent medium inhomogeneities along the path of beam propagation is obtained from measurements of the phase of the wave coming from a reference source.

A reference source, interpreted as an object with known amplitude–phase distribution placed at a known distance, can be formed directly at the surface of an object analyzed within optical system. It may also be an infinitely far light source (a star) or the one placed between the object and the telescope.[9]

Let us consider the following experiment (Fig. 4): when an extended object is placed in the plane x_{obj}, a point reference source – in the plane x_{ref} and a receiving telescope – in the plane x_0. The telescope will be described with an equivalent lens of the aperture $W(\rho)$ contributing to the phase with the term $\exp(-ik\rho^2/2f)$, where f is the focal length of the telescope. Since the reference source is assumed to be a point source emitting coherent light the wave phase in the plane x_0 can be expressed as

$$S_{ref}(x_0, \rho) = k\rho^2/2 \, (x_{ref} - x_0) + S(x_0, \rho; x_{ref}, 0) \, ,$$

where S is the random phase of a spherical wave induced by turbulence when it propagates from x_{ref} to x_0.
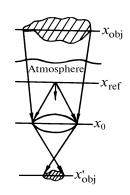

FIG. 4. Optical arrangement of an experiment involving an extended object, reference source, telescope, and the image plane.

In the case of a vertical path in order to provide maximum efficiency the reference source must be placed above the effective layer of a turbulent atmosphere.

To correct for distortions, we use an algorithm of phase conjugation. Then the corrected field in the image plane x'_{obj} takes the form

$$U_{im}(x'_{obj}, \rho) = \int \int d^2\rho_1 d^2r_1 U_{obj}(r_1) W(\rho_1) \exp(-i\,kr_1^2/2\,f) \times$$

$$\times G_0(x'_{obj}, \rho; x_0, \rho_1) G(x_0, \rho_1; x_{obj}, r_1) \exp(-i\,S(x_0, \rho_1; x_{ref}, 0)), \quad (38)$$

where $U_{obj}(\rho_1)$ is the object's field distribution, r_1 is the variable of the integration over the object, and ρ_1 is the variable of integration over telescope aperture. We use in our calculations the following expression for the structure function of phase:

$$D_s(x, \rho; x', \rho') = 2.91 k^2 \int_{x'}^{x} d\xi \, C_n^2(\xi) \left| \frac{(\xi - x')}{(x - x')} r + \frac{(\xi - x)}{(x - x')} r' \right|^{5/3}. \quad (39)$$

The structure characteristic of the refractive index C_n^2 in Eq. (39) depends on the variable of integration over the path.

The optical transfer function for the system "telescope–atmosphere" is introduced by

$$\langle I(f, \rho) \rangle = \frac{k^2}{4\pi^2 f^2} \int \int d^2r \, \langle \tau(r) \rangle \exp(-i\,k\,r\,\rho) \, . \quad (40)$$

Here $\langle I(f, \rho) \rangle$ is the average intensity distribution in the image plane. Calculations for a Gaussian aperture $(W(\rho) = \exp(-\rho^2/2R^2))$ give

$$\langle \tau(r) \rangle = \pi R^2 \frac{\Omega_{obj}^2}{(1 + \Omega_{obj}^2 + \Omega_R \Omega_{obj} + 4\Omega_{obj}/\Omega_a)} \times$$

$$\times \exp \left\{ -\frac{r^2}{4R^2} \left[1 + \frac{4\Omega_R}{\Omega_{eff}} + \frac{\Omega_R \Omega_{obj}(1 + \Omega_{obj}/\Omega_a)}{(1 + 4\Omega_{obj}/\Omega_a + \Omega_{obj}^2)} + \right. \right.$$

$$\left. \left. + \frac{\Omega_R^2 (1 + 4\Omega_{obj}/\Omega_a)^2}{(1 + 4\Omega_{obj}/\Omega_a + \Omega_{obj}^2)(1 + 4\Omega_{obj}/\Omega_a + \Omega_{obj}^2 + \Omega_R \Omega_{obj})} \right] \right\} \, , \quad (41)$$

where

$$\Omega_a = \frac{k\,r_a^2}{x_{obj} - x_0} \, ; \quad \Omega_{obj} = \frac{k\,a_{obj}^2}{(x_{obj} - x_0)} \, ;$$

$$\Omega_R = \frac{k\,R^2}{x_{obj} - x_0} \, ; \quad \Omega_{eff} = \frac{k\,r_{eff}^2}{(x_{obj} - x_0)} \, ;$$

$$r_a = \frac{x_{obj}}{x_{ref} - x_0} \, (2.68\,k^2 \int_{x_0}^{x_{ref}} d\xi \, C_n^2(\xi))^{-3/5} \, , \quad (42)$$

a_{obj} is the object size; r_a is the size of isoplanarity zone of the atmosphere; and, r_{eff} is the effective coherence length determined by the atmospheric inhomogeneities above the reference source. By definition (Eq. (42)) the isoplanarity zone is seen in the object plane at the same angle as the coherence length of the effective atmospheric layer is seen through this layer.

Therefore, the optical transfer function (41) depends essentially on the ratio of the telescope size and the effective coherence length $(\Omega_R/\Omega_{eff} = R^2/r_{eff}^2)$ and on the ratio of the dimensions of an object and isoplanarity zone $(\Omega_{obj}/\Omega_a = a_{obj}^2/r_a^2)$ as well as on their combination.

With the help of introduced optical transfer function one can calculate the resolution of the whole "telescope–atmosphere" optical system

$$\Re = \int \int d^2 \kappa <\tau(\kappa)> , \qquad (43)$$

where $\kappa = kr/f$ is a spatial frequency. From Eqs. (41) and (43) for the case $\Omega_{obj} \gg \Omega_R$, $\Omega_{obj} \gg 1$, and $\Omega_{eff} \gg \Omega_R$ we obtain

$$\Re = 2\pi k^2/f^2 [1/R^2 + 4/r_a^2 + 4/r_{eff}^2]. \qquad (44)$$

So, the resolution is determined by the minimum value among the set of telescope size R, effective coherence length r_{eff}, and isoplanarity length r_a. Given the telescope size and the object altitude which determines the isoplanarity length r_a, one can increase r_{eff} by choosing the position x_{ref} of the reference source. If the reference source is at the object we obtain infinite value of r_{eff}, and

$$\Re = 2\pi k^2/f^2 (1/R^2 + 4/r_a^2) . \qquad$$

In this case resolution is limited by the size of the isoplanarity zone.[9]

In conclusion of this section let us note that the efficiency of an atmospheric adaptive optical system using a reference source can be significantly increased. Altitude of the reference source position is determined by both the shape of C_n^2 profile along the path of propagation and the equation of admissible residual distortions still providing image formation. Optical system provides aberrationless image of the isoplanar zone only. Proper choice of a reference source position can bring the resolution of the optical system to an ultimate value determined by the length of isoplanarity zone. Therefore altitude values for which $r_a > R$ provide a diffraction limited resolution.

7. DYNAMIC CHARACTERISTICS OF THE ADAPTIVE OPTICAL SYSTEMS (1984)

As known, the adaptive optical system being a system with a feedback has a finite response time and, as a result, a limited frequency band pass. In this section we investigate[10] the influence of a delay time on the efficiency of an adaptive system operation. To evaluate the quality of correction, we use Strehl parameter (i.e., relative change in axial intensity).

If the transition processes in a feedback loop of an adaptive system are ignored, it can be considered as a system with a constant delay time τ which can be interpreted as a response time of an adaptive circuit. This means that because of this delay time we make a control of the adaptive system based on the preceding measurements of the phase of a reference source field. Thus, a problem arises on estimating an admissible delay time τ and corresponding frequency pass band Δf of a feedback loop of the whole adaptive system.

Using the phase approximation of a Huygens–Kirchhoff method, we can write the average axial intensity of the corrected field as follows:

$$<I(0, \tau)> = \frac{1}{\lambda^2 l^2} \int \int d^4\rho_{1,2} A(\rho_1) A^*(\rho_2) \exp\left(-i k \frac{(\rho_1^2 - \rho_2^2)}{2 l}\right) \times$$

$$\times <\exp \{i [S(0, \rho_1; l, 0; t + \tau) - S(0, \rho_2; l, 0; t + \tau)] -$$

$$- i [S(0, \rho_1; l, 0; t) - S(0, \rho_2; l, 0; t)]\}> . \qquad (45)$$

Here $A(\rho)$ is the initial distribution of field, l is the distance passed by the wave in a randomly inhomogeneous medium, t is current time, and τ is the constant delay time. Everywhere below we shall use brief notation $S(\rho, t)$ instead of $S(0, \rho; l, 0; t)$ for the phase fluctuations of a spherical wave.

Using the hypothesis of frozen phase fluctuations, i.e.,

$$S(\rho, t + \tau) = S(\rho + \mathbf{v} \tau, t) ,$$

($\mathbf{v}$ is the vector of wind velocity), after some calculations[10,11] we obtain

$$<I(0, \tau)> = \lambda^{-2} l^{-2} \int \int d^4\rho_{1,2} A(\rho_1) A^*(\rho_2) \times$$

$$\times \exp\left(- i k \frac{(\rho_1^2 - \rho_2^2)}{2 l} - 12 <a_4^2> \frac{\tau^2 v^2}{R^4} (\rho_1 - \mathbf{r}_2)^2\right) , \qquad (46)$$

where

$$<a_4^2> = 0.074 (R / r_0)^{5/3} ,$$

for Kolmogorov turbulence R is the radius of the phase expansion circle, namely, radius of the receiving aperture of a telescope or an optical beam. For example, when focusing the beam through the turbulent atmosphere[11] we have

$$<I(0, \tau)> = \Omega^2 (1 + 3.52 \tau^2 v^2 r_0^{-5/3} a^{-1/3})^{-1} .$$

The correction will be efficient if

$$\tau \ll (r_0/v) (a/r_0)^{1/6} , \qquad (47)$$

where r_0 is radius of coherence for a spherical wave, $\Omega = k a^2/l$, and $v = |\mathbf{v}|$.

A stepwise control function with the delay time τ corresponds to a frequency spectrum of the form $\sin(\pi f\tau)/(\pi f\tau)$. So, if we take the first zero of $\sin x/x$ function for the frequency band width then for the frequency band width of the feedback loop we obtain

$$\Delta f \sim 1/\tau \gg (v/r_0) (r_0/a)^{1/6} . \qquad (48)$$

It should be noted that in addition to the system with a constant delay time, a system can be proposed in which a correcting phase at the moment $t + \tau$ is formed as the forecast

$$\hat{S}(\rho, t + \tau) = S(\rho, t) + \nabla_\rho S(\rho) \mathbf{v} \tau . \qquad (49)$$

An acceptable delay time τ_1 is then given by

$$\tau_1 \gg (r_0/v) (a/r_0)^{7/12} . \qquad (50)$$

A comparison of Eqs. (47) and (50) shows that if a correction uses measurements not only of the phase but of its derivatives $\left(\frac{\partial S}{\partial y}, \frac{\partial S}{\partial z}\right)$, it remains efficient for much longer delay time τ_1:

$$\tau_1 / \tau = (a/r_0)^{5/12} . \qquad (51)$$

Eq. (51) shows that adaptation based on algorithm (49) admits much longer delay time. The stronger are the phase distortions (i.e., the greater is the ratio a/r_0), the longer is the time gain in comparison with usual adaptation scheme.

The correction method in accordance with Eq. (49) is rather practicable because the phase meters usually measure not the phase itself but its derivative or phase difference.

8. FORECASTING ADAPTIVE SYSTEMS (1985)

The next stage in the development of the theory of atmospheric adaptive optical systems was introduction[11] of a new class of forecasting systems.

When comparing different dynamic modes[11] of operation of adaptive optical systems, we deal with the problem on how to extrapolate currently measured phase to subsequent time moments. It can be however treated as the problem on forecasting random optical wave phase at the moment $t + \tau$ based on measurements performed at the moment t.

Let us compare three different methods of forecasting. We will use the symbol ˆ to indicate the forecasted value.

1) The forecast of random value $S(\mathbf{r}, t + \tau)$ from its average. In fact, such an adaptive system does not provide any correction $\hat{S}(\mathbf{r}, t + \tau) = <S(\mathbf{r}, t)> = m$. As a rule, the average m equals zero.

2) The forecast based on the last (current) measured value. This method corresponds to adaptive correction with a constant delay time $\hat{S}(\mathbf{r}, t + \tau) = S(\mathbf{r}, t)$.

$$\hat{S}(\mathbf{r}, t + \tau) = S(\mathbf{r}, t) .$$

3) The statistical forecast based on a set of previously measured values $\hat{S}(\mathbf{r}, t + \tau) = b_S(\tau) S(\mathbf{r}, t)$. Here $b_S(\tau)$ is the normalized time correlation function of the phase fluctuations.

The quality of the forecast will be determined from statistical moments of deviations of the forecasted variable from its true value. For example, the variance[3]

$$<e^2> = <[S(\mathbf{r}, t + \tau) - \hat{S}(\mathbf{r}, t + \tau)]^2>$$

will determine the quality of the field average forecast. For the three methods described above we have respectively

$$<e^2>_1 = s_S^2 ,$$

$$<e^2>_2 = 2 s_S^2 [1 - b_S(\tau)] = D_S(v\ \tau) ,$$

$$<e^2>_3 = \sigma_S^2 [1 - b_S^2(\tau)] ,$$

where σ_S^2 is the variance of phase fluctuations and $D_s(v, \tau)$ is the structure phase function. Figure 5 shows, for a comparison, the dependence of the refractive forecast variance $<e^2>/\sigma_S^2$ on the delay time τ. We see that the error of forecasting the field average[3,11] depends both on the variance and time scale of phase fluctuations. Obviously the third (statistical) method provides better correction in comparison with the other two at any τ.
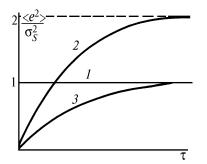

FIG. 5. *Relative variance of the forecast: 1)* $<e^2>_1/\sigma_S^2$ *(1st forecast method), 2)* $<e^2>_2/\sigma_S^2$ *, and 3)* $<e^2>_3/\sigma_S^2$ *.*

As to the correction of the average intensity distribution,[3] its efficiency will be determined by the following value:

$$<\beta^2> = <\{[S(\mathbf{r}_1, t + \tau) - \hat{S}(\mathbf{r}_1, t + \tau)] - [S(\mathbf{r}_2, t + \tau) - \hat{S}(\mathbf{r}_2, t + \tau)]\}^2> .$$

Once the variances for all three correction methods are calculated we obtain

$$<\beta^2>_1 = D_S(|\mathbf{r}_1 - \mathbf{r}_2|) , \quad <\beta^2>_2 = 2D_S(|\mathbf{r}_1 - \mathbf{r}_2|) - 2B_{\Delta S}(\tau) ;$$

$$<\beta^2>_3 = D_S(|\mathbf{r}_1 - \mathbf{r}_2|) (1 + b_S^2(\tau)) - 2b_S(\tau) B_{DS}(\tau) .$$

It is seen from these expressions that in order to evaluate correction errors for different forecasts one should be able to calculate the structure function of phase and time correlation function of the phase difference fluctuations

$$B_{DS}(\tau) = \frac{1}{2} D_S(|(\mathbf{r}_1 - \mathbf{r}_2) + \mathbf{v}\tau|) + \frac{1}{2} D_S(|(\mathbf{r}_1 - \mathbf{r}_2) - \mathbf{v}\tau|) - D_S(|\mathbf{v}\tau|) .$$

Let us then consider how to forecast the phase fluctuations using the expansion of phase over modes. Let the aperture be a circle with the radius R, then the wave phase can be expanded over polynomials $F_j(\mathbf{r}/R)$, orthonormal within the circle

$$S(\mathbf{r}, t) = \sum_{j=1}^{\infty} a_j(t) F_j(\mathbf{r}/R) ,$$

where a_j are the expansion coefficients. Based on this expansion obtained from measurements performed at the moment t, we can write the statistical forecast for the moment $t + \tau$ as follows:

$$\hat{S}(\mathbf{r}, t + \tau) = \sum_{j=2}^{\infty} a_j(t) b_j(\tau) F_j(\mathbf{r}/R) ,$$

where $b_j(\tau)$ are normalized correlation functions. It is easy to show that comparatively the efficiency of the third method (compared to the second one) will be proportional to $(1 - b_j(\tau))^{-2}$ for the mode component of the number $j = 2$, $3, \dots$. The greater is the mode number j, the smaller is the spatial correlation radius: the largest radii have random phase tilts ($j = 2, 3$), defocusing and astigmatism ($j = 4, 5, 6$) have smaller radii, then coma comes ($j = 7, 8$), and so on. At a fixed τ the efficiency of the mode statistical forecast, being proportional to $(1 - b_j(\tau))^{-2}$, grows with the increase of j.

Based on modified atmospheric models, we have calculated dynamic parameters of an adaptive ground–based telescope.[16] We have compared (see Fig. 6) Strehl parameter St for different adaptive systems: curves *1* correspond to a telescope without a correction, *3* — a system with an constant delay time, and *4* — a system using the forecast by Eq. (49). Corresponding curves with different values of D/r_0 ratio are shown in Fig. 6. Curves *2* correspond to asymptotic calculation of Strehl parameter[11,16] in the systems with $\hat{S}(\mathbf{r}, t + \tau) = S(\mathbf{r}, t)$ according to the formula

$$St(\tau) = St + \exp (- D_S(\mathbf{v}\tau)) [1 - St] ,$$

where St is Strehl parameter for a system without a correction. It is seen from the last expression that $St(\tau) \to 1$ for $D_S(v\tau) \to 0$ whereas for $D_S(v\tau) \to \infty$ $St(\tau) \to St$, i.e., to the parameter characteristic of a system without correction.
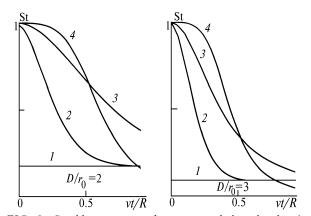

FIG. 6. Strehl parameter for a ground–based adaptive telescope as a function of generalized parameter $v\tau/R$. Figures at the curves are explained in the text.

9. MODE CORRECTION FOR TURBULENT DISTORTIONS OF THE OPTICAL WAVES (1985)

Creation of a highly sophisticated adaptive optical system providing for real time correction of all distortions is quite a complicated technical problem. In this connection an idea of forming corrected optical wave without adaptive mirror seems to be rather fruitful especially at the stage of development.

Thus, in Ref. 12 we have shown how to imitate mode correction based on the analysis of phase structure of the optical wave passed through a turbulent medium either directly or with the help of a corner–cube reflector. Assume that all turbulent fluctuations are reduced to the phase ones, then for the directly propagated wave we have

$$U_1(\mathbf{r}) = \exp\left(i\,S(\mathbf{r})\right), \qquad (52)$$

whereas for the reflected wave that twice passes a medium layer (after reflection from a corner–cube reflector)

$$U_2(\mathbf{r}) = \exp\left(i\,S(\mathbf{r}) + i\,S(-\mathbf{r})\right). \qquad (53)$$

Calculation of the mutual coherence functions for the fields described by Eqs. (52) and (53) using expansion of $S(\mathbf{r})$ over orthogonal polynomials gives[12]

$$\Gamma_1(\mathbf{r}_1, \mathbf{r}_2) = \exp\left\{-3.44(\left|\mathbf{r}_1 - \mathbf{r}_2\right| / r_0)^{5/3}\right\}, \qquad (54)$$

$$\Gamma_2(\mathbf{r}_1, \mathbf{r}_2) = \exp\left\{-0.54\,R^{-7/3}\,r_0^{-5/3}\left[3(r_1^4 + r_2^4) - 4r_1^2\,r_2^2\right]\right\}. \qquad (55)$$

Comparison of Eqs. (54) and (55) shows that the reflected field is coherently anisotropic in contrast to the direct one. Equation (55) also shows that for a corner reflector of the size $R \gg r_0$ the reflected wave restores its coherence during the backward propagation almost completely.

This result can be treated not in terms of the direct and reflected waves but as a result of adaptive mode correction of phase distortions of the reflected wave. The adaptive correction is done by introducing phase predistortions into the initial distribution. In this case the field, corrected according to phase conjugation method, is

$$U_c(\mathbf{r}) = \exp\left\{i\,S(\mathbf{r}) - i\,S_c(\mathbf{r})\right\}, \qquad (56)$$

where $S_c(\mathbf{r}) = -S(-\mathbf{r})$. As a result the field (56) coincides with that given by Eq. (53) which assumes the use of a corner reflector. Therefore, the use of a corner reflector simulates the phase conjugation mode correction method with antisymmetric modes being under correction.[12]

We have performed experimental verification of this analysis. Some results of the coherence measurements are presented in Figs. 7 and 8. Pairs of curves 1 and 2 and 3 and 4 are obtained at different turbulence regimes such that a five–fold difference in the coherence radii could be observed. Comparison of curves 1 and 2 and 3 and 4 shows that mode correction of phase distortions essentially raises the coherence of radiation. Figure 8 confirms the result of Ref. 12 on a strong coherence anisotropy in the wave where antisymmetric modes of phase fluctuations are corrected.

FIG. 7. Comparison of coherence functions for direct and reflected radiation: curves 1 and 3 — direct radiation at different turbulence regimes and curves 2 and 4 — the same for reflected radiation.

FIG. 8. Anisotropy of the coherence function for reflected radiation: curves 1 and 2 — coherence functions for direct radiation and curves 3 and 4 — the same for reflected radiation; curves 1 and 3 refer to central spacing of observation points whereas curves 2 and 4 refer to the symmetric spacing.

Thus the experiments on the mode correction well confirm theoretical results. Efficiency of this rather complicated optical phase correction can be estimated from

comparative measurements of coherence of both direct and reflected waves.

10. EFFICIENCY OF A TWO–COLOR ADAPTIVE OPTICAL SYSTEM (1978, 1986)

The adaptive optical system as a system with the feedback loop closed optically through the atmospheric layer uses for its control the data of optical measurements in the fields produced by reference sources. This usually implies that reference and corrected sources emit at the same wavelength.

However, for some practical applications it is worthwhile to use the initial and reference radiation of different wavelengths. Such a two–color adaptive system was first considered in Ref. 15 where the expression for structure function of the phase difference of two spherical waves was obtained.

In this section we investigate the behavior of eikonals difference for two optical waves, following Ref. 13. It is known that variation of eikonal $\Theta(\rho, k)$ at the wavelength λ ($k = 2\pi/\lambda$), being equal to $S(\rho, k)/k$, represents linear variation of the optical paths difference. Note that adaptive mirrors correct precisely these linear variations but not the phase distortions measured in radians.

To analyze the influence of frequency decorrelation on the efficiency of two–color adaptive optical system, let us examine statistical parameters of eikonals difference fluctuations for two wavelengths λ_1 and λ_2. In the approximation of smooth perturbations method the eikonal variations for the plane wave[2] are

$$\Theta(\rho, k) = \int\limits_0^L dx \int\int d^2n\,(\kappa, x)\,e^{i\kappa\rho} \cos\left[\frac{k^2(L-x)}{2\,k} \right], \quad (57)$$

where L is the distance and $d^2n(\kappa, x)$ is spectral amplitude of fluctuations of the refractive index $n_1(\mathbf{r})$. It is given by formula

$$n_1(\mathbf{r}) = \int\int d^2n\,(\kappa, x) \exp\,(i\,\kappa\,\rho)\,.$$

Let us first calculate the variance of eikonals difference (57) for wavelengths λ_1 and λ_2

$$\sigma_{\Delta\Theta}^2 = 2\pi^2 \int\limits_0^L dx \int\limits_0^\infty d\kappa\,\kappa\Phi_n(\kappa) \left[\cos\frac{k^2(L-x)}{2\,k_1} - \cos\frac{k^2(L-x)}{2\,k_2} \right]^2 \quad (58)$$

for the turbulence spectrum of the form

$$\Phi_n(\kappa, x) = 0.033\,C_n^2(x)\,(\kappa^2 + k_0^2)^{-11/6} \exp\,(-\,\kappa^2\,/\,k_m^2)\,,$$

where κ_0 and κ_m are the wave numbers for the outer and the inner turbulence scales. We have performed numerical calculations[16,18] according to Eq. (58) for the case of vertical propagation of radiation in the atmosphere. We have chosen a vertical profile of atmospheric turbulence intensity in the form

$$C_n^2(h) = C_n^2(0) \begin{cases} (1 + h/h_0)^{-2/3}, & h \le h_1, \\ (h/h_1)^{-4/3}(1 + h_1/h_0)^{-2/3}, & h > h_1, \end{cases} \quad (59)$$

where $h \in [0, L]$. The values of the parameters used are as follows: outer scale $2\pi/\kappa_0 = 100$ m, inner scale $5.92/\kappa_m = 0.01$ m, path length $L = 1000$ m, heights

$h_0 = 30$ m, $h_1 = 300$ m, and coherence radius $r_0 = 0.1$ m at the wavelength of 0.55 μm.

Results of calculations are presented in Table II. Numbers in the first column indicate the wavelength where correction is executed (a reference wave), while in the second column the wavelength of corrected radiation is given, the third column gives the values of corresponding variances $\sigma_{\Delta\Theta}^2$.

TABLE II.

λ_1, μm	λ_1, μm	$\sigma_{\Delta\Theta}^2 \cdot 10^3$, μm
0.5	1.0	4.44
0.5	2.0	8.06
0.5	3.0	10.4
0.5	4.0	12.2
0.5	5.0	13.7
0.5	6.0	15.0
0.5	7.0	16.2
0.5	8.0	17.3
0.5	9.0	18.3
0.5	10.0	19.2

These results correspond to the outer turbulence scale $2\pi/\kappa_0 = 100$ m. We have also performed calculations for the vertical profile $2\pi/\kappa_0 = 2\sqrt{h}$ with the results appeared to be practically identical to those in Table II. So the variance of eikonals difference for two different wavelengths is insensitive to variations of the outer turbulence scale. At the same time, $\sigma_{\Delta\Theta}^2$ is rather sensitive to changes in the inner turbulence scale and in the path length. Table III shows the dependence of $\sigma_{\Delta\Theta}^2$ on changes in the inner turbulence scale at path 1000 m long.

TABLE III.

Inner scale of turbulence, $5.92/\kappa_m$, m	0.03	0.01	0.003
$\sigma_{\Delta\Theta}^2$, μm	0.017	0.019	0.020

Table IV presents the dependence of σ_{DH}^2 on the path length at the inner turbulence scale of 0.01 m.

TABLE IV.

Path length L, m	1000	3000	6000	10000
$\sigma_{\Delta\Theta}^2$, μm	0.0192	0.0256	0.0299	0.0346

Therefore, our results prove the efficiency of the two–color adaptive correction[13,15,16] to be high over a wide wavelengths range.

11. ELEMENTS OF ADAPTIVE OPTICS (1984, 1987)

It is known that wave–front corrector is the basic element of any adaptive system. Efficient correctors of the wave front tilts for adaptive systems operating in a turbulent atmosphere should satisfy the following demands: high operation speed, high enough spatial resolution, and a wide dynamic range of angular deflectors of radiation at significant mass and size of movable optical elements. To construct such a corrector is nowadays quite a complicated technological problem.

In the known constructions of deflectors the speed of about 10^{-2}–10^{-3} s is provided only for small optical

elements which makes them useful in operations only with narrow beams (not exceeding 10 mm in diameter).

In this section we describe[14] the passive–active bimorph deflector that uses a piezoceramic compensator to control angular orientation of an optical element (a mirror) of 50–g mass, in the range of angles up to 60″, with the frequency up to 100 Hz. The square bimorph element is formed by two polarized piezoceramic disks with thickness of 1 mm made of ZTS–19 material.

At the next step[18] we constructed a 19–element compound mirror with hexagonally packed elements. It is precisely this packing that allows most abutting arrangement of the elements with minimum diffraction losses at their edges, and it also provides for the best filling of a round aperture.

For the base of this compound mirror we used a thick glass plate with installation packets for 19 piezoceramic cylinders 17.4 mm in diameter. The packets keyways were cut by means of a diamond–tipped tool. The mirror elements are made in the form of hexagons from an optical glass 5 mm thick and about 15 mm in optical diameter. The reflecting surfaces are aluminium coated. Elements are attached to cylinders with the elastic optical cement.

The actuators of a compound mirror are the piezoceramic ZTS–19 cylinders. They provide linear displacement of optical elements in the range $\pm 5\lambda$ (where $\lambda = 0.63$ μm) with the control voltage of ± 500 V and speed of about 10 ms.

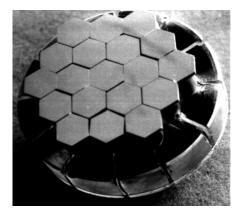The view of 19–element mirror is presented in Fig. 9.

FIG. 9. Photo of the 19–component compound mirror.

To control the elements of a compound mirror in axial and two angular coordinates, we have designed an actuator using the piezoceramic cylinder with split electrodes at the surface. Control voltages are formed using signals from wave front sensors by means of special high–voltage amplifiers.[14,20]

These elements are used in experiments on correction of beams and images in the turbulent atmosphere.

12. EFFICIENCY OF CORRECTION FOR COMMON TILTS AND DEFOCUSING OF THE WAVE FRONT (1988)

A diagram of an optical experiment is presented in Fig. 1. It must form an image of a remote object by means of the main mirror and an adaptive element which corrects a received wave front for aberrations. Besides, it performs the adaptive focusing of laser radiation on an object behind the medium layer.

A device measuring moments of intensity distribution of the optical field in the focal plane is proposed[19] here as a

wave–front sensor generating a control signal for the adaptive optical element. This "moments meter" measures values of the following functionals:

$$M_y = \frac{\int\int d^2r\, y\, I(F, \mathbf{r})}{\int\int d^2r\, I(F, \mathbf{r})} \,, \quad M_z = \frac{\int\int d^2r\, z\, I(F, \mathbf{r})}{\int\int d^2r\, I(F, \mathbf{r})} \,, \quad (60)$$

$$M_{yy} = \frac{\int\int d^2r\, y^2\, I(F, \mathbf{r})}{\int\int d^2r\, I(F, \mathbf{r})} \,, \quad M_{zz} = \frac{\int\int d^2r\, z^2\, I(F, \mathbf{r})}{\int\int d^2r\, I(F, \mathbf{r})} \,, \quad (61)$$

where $I(F, \mathbf{r})$ is the field intensity distribution in the focal plane.

Based on the results of moments measurements, we may now construct a phase $\hat{S}(0, \mathbf{r})$ which provides for its best correction $S(0, \mathbf{r})$ describing the phase distortions of the wave front at the receiving aperture. This may be, for example,

$$\hat{S}(0, \boldsymbol{\rho}) = \frac{k}{F}\,(M_y\, y + M_z\, z) + \frac{1}{2}\left(\frac{k}{F}\right)^2 (M_{yy}\, y^2 + M_{zz}\, z^2) \,.$$
(62)

Here the phase providing the correction $\hat{S}(0, \boldsymbol{\rho})$, see Eq. (62), implies that adaptive element controls common tilts along two coordinate axes and wave front curvature in two directions. In real experiments the first two summands in Eq. (62) correspond to inclinations of a flat mirror whereas the other two summands imply use of two flexible mirrors, each changing its curvature only in one direction. One can use also two crossed cylindrical lenses.

To estimate the efficiency of this correction algorithm, consider the following structure function:

$$D(\boldsymbol{\rho}_1, \boldsymbol{\rho}_2) = <\{[S(0, \boldsymbol{\rho}_1) - \hat{S}(0, \boldsymbol{\rho}_1)] - [S(0, \boldsymbol{\rho}_2) - \hat{S}(0, \boldsymbol{\rho}_2)]\}^2>. \quad (63)$$

Here angular brackets mean averaging over an ensemble of random field values, and we use expansion of the random phase over orthogonal polynomials. The first term to be accounted for in Eq. (63) corresponds[19] to

$$D_1(\boldsymbol{\rho}_1, \boldsymbol{\rho}_2) = \frac{24}{5}\,<a_5^2>\,(y_1\, z_1 - y_2\, z_2)^2 \,, \qquad (64)$$

where $<a_5^2>$ is the variance of fluctuations of the wave front astigmatism. For the Kolmogorov model of turbulence spectrum

$$<a_5^2> = 2.32 \cdot 10^{-2}\,(2R/r_0)^{5/3} \,.$$

Our calculations[19] show that adaptive correction (62) of common tilts and defocusing makes the equivalent coherence radius 9.3 times larger.

13. ADAPTIVE OPTICAL SYSTEM TO CORRECT FOR IMAGE DISTORTIONS (1988)

The first use of the simplest algorithm of adaptive correction of images constructed through the atmosphere has been described in Ref. 20. The adaptive optical system presented here should correct the image of an optical source for distortions due to random tilts of radiation wave front during its propagation through the turbulent atmosphere.

To perform an image correction algorithm we have built an experimental setup schematically shown in Fig. 10. The setup consists of a transmitting part, atmospheric path, measuring channel and a correction channel.
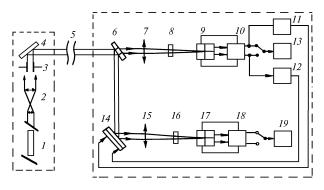

FIG. 10. Block diagram of an experimental setup: 1 — laser, 2 — collimator, 3 – diaphragm, 4 — rotating mirror, 5 — atmospheric path, 6 — beam–splitting plate, 7 and 15 — lenses, 8 and 16 — optical filters, 10 and 18 — processing units, 11 and 12 — amplifiers, 13 and 19 — spectrum analyzers, 14 — active mirror, and 9 and 17 — coordinate photodetectors.

The transmitting part consists of a He–Ne laser 1; its radiation is shaped by a collimator 2 and a diaphragm 3. The atmospheric path 5 of length $L = 100$ m is at 10 m altitude above the ground. The laser beam of 1–cm diameter after passing the atmospheric path is splitted at the input of a receiving system. The first beam passes through an optical wedge 6 and comes to a measuring channel; the second beam reflected from the front surface of a wedge 6 comes to a correction channel.

In the measuring channel the lens 7 forms an image of the source. The quadrant coordinate–sensitive photodetector 9 is placed in the focal plane of the lens 7. The processing unit 10 generates signals proportional to coordinates of the random position of center of gravity of the beam. Special amplifiers[20] with the pass band of 0– 2 kHz have the dynamic range of 60 dB. The threshold angular displacement of the image center, still measured by the system, is $3.1 \cdot 10^{-7}$ rad. Compensation for random displacements of image is performed[14] by means of an active mirror 14. Choosing the gains we control the laser beam inclination in a way enabling us to form an image corrected for angular shifts of the source in the focal plane of the lens 15.

The correction efficiency was examined with the methods of spectral analysis. We considered the temporal spectra of the image random gravity center displacements. The quality of correction was evaluated by the quantity

$$E_{y,z}(f) = [S_{y,z}(f) \, / \, S_{y,z}^{a}(f)]^{1/2} , \qquad (65)$$

where $S_{y,z}^{a}(f)$ and $S_{y,z}(f)$ are the spectral power densities of the random axial displacements of an image energy gravity center in a system with and without an adaptive correction, respectively. Measurements were performed successively in three frequency ranges: 0.05–2 Hz, 0.5–20 Hz, and 5–200 Hz.

Figure 11 shows frequency dependences of the efficiency of correction for angular displacements (65) in two perpendicular planes $E_y(f)$ and $E_z(f)$. It is seen that correction efficiency along both coordinates of the image gravity center is between 4 and 12. The greater is the

frequency of random displacements of the center, the lower is the efficiency. These dependences show dynamic potentialities of this adaptive optical system.
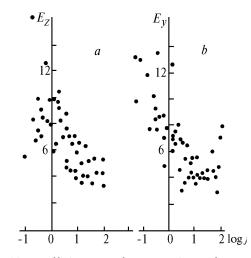

FIG. 11. Efficiency of correction for angular displacements of image gravity center along Y–axis (a) and along Z–axis (b).
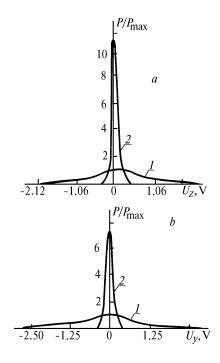

FIG. 12. Probability distribution of the signal, proportional to random displacement of the gravity center along Y (a) and Z (b) axes with (curve 2) and without (curve 1) adaptive image correction. Here P_{max} is maximum of the probability distribution in the case of no correction.

The total over the frequency range efficiency of an adaptive image correction can be estimated from a comparison of histograms. With the help of histograms we have derived the rms deviations and calculated the values of $M_{y,z} = \sigma_{y,z} / \sigma_{y,z}^{a}$ (here $\sigma_{y,z}^{a}$ and $\sigma_{y,z}$ are the rms deviations of random center displacements of images with and without correction). Our results are $M_y = 5.3$ and

$M_z = 7.4$. For a convenience of the comparison, Fig. 12 gives superimposed probability distributions for the analyzed signals in the systems with and without correction, in dependence on measured voltages U_z and U_y.

Thus, the performed investigations have shown good efficiency of image correction by means of an adaptive optical system.[20]

14. MULTICOMPONENT SYSTEM OF IMAGE CORRECTION (1990)

In this section we consider[21] efficiency of a combined adaptive four–component mirror each element of which corrects tilts in two orthogonal directions only.

At present it is acknowledged that it is worth using systems compensating for image displacements as a primary system of adaptive correction in telescopes. Such systems use, as a rule, sensors that measure coordinates of an image center of gravity. There already exists a number of telescopes using compensation for image gravity center displacements. Actually, this means constructing of a high precision teleguide which now is incorporated in most telescopes.

The next stage of development of adaptive optical systems is correction for higher–order aberrations of the phase front. It requires some special equipment: the wave–front sensor and the controlled active (adaptive) mirror. The use of two types of mirrors is possible: the compound one performing zonal correction and the flexible one enabling the performance of mode correction for the phase front aberrations.

Since we use a four–component mirror, it is natural that the wave–front sensor should have four identical meters measuring gravity center of image within the limits of each subaperture.[20]

The possible arrangement of an optical experiment is shown in Fig. 13. The first loop of the adaptive correction for the displacements of the gravity center as a whole is provided by the first adaptive element A_1. If the aperture of an image–forming optical device is considered as a circle of radius R, then the wave phase after angular correction can be expressed in terms of the following expansion over Zernike polynomials:

$$S_1(\mathbf{r}) = \sum_{j=4}^{\infty} a_j F_j(\mathbf{r}/R) , \qquad (66)$$

where $F_j(\mathbf{r}/R)$ are Zernike polynomials and a_j are the phase coefficients. The first term $a_1 F_1(\mathbf{r}/R)$ in Eq. (66) is omitted because it does not affect the phase fluctuations in the image. The second stage of the adaptation includes measuring of local wave front tilts in the limits of subapertures and their correction by means of the four–component mirror A_2.

Before proceeding to calculations, let us investigate the physical structure of different stages of the adaptive correction shown in Fig. 13. If the initial wave phase is a plane, then an image formed by the optical system (or by an equivalent lens) presents the Airy diffraction picture. The phase aberrations spread the image. After the first correction with the help of element A_1, the formed image is center–stabilized but the phase aberrations like astigmatism and defocusing still remain. These aberrations surely make the local tilts to appear within each of the subapertures.
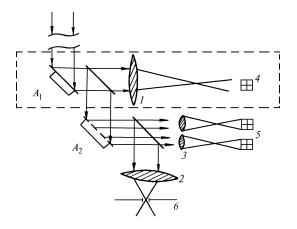

FIG. 13. Arrangement of an optical experiment: 1 and 2 – lenses, 3 – four–lens unit, 4 – coordinate photodetector, 5 – unit of four coordinate–sensitive photodetectors, and 6 – image photorecorder.

It should be noted that account for defocusing solely in the phase of Eq. (66) suggests that correction of random tilts at each segment of a four–component mirror makes its surface to be a side of a quadrangular prism which reflects waves in four directions.

Let us examine the efficiency of correction using such a compound mirror. Let the initial lens forming the image have a Gaussian aperture, and compare the focal plane intensity distribution in three most typical cases: 1) propagation of radiation in vacuum, 2) presence of aberrations like defocusing with corrected common tilts, and 3) the defocusing corrected by means of a compound four–component mirror.

In the case 1 intensity distribution is

$$I_1(F, \rho) = \Omega^2 \exp(-\rho^2 \Omega^2 / R^2) ,$$

where $\Omega = kR^2/F$, while the initial Gaussian aperture is

$$A(\rho) = \exp(-\rho^2/2R^2) .$$

In the case 2 the average intensity distribution is

$$\langle I_2(F, \rho) \rangle = \frac{\Omega^2}{2R^2} \int_0^\infty dr \, r \, \frac{\exp(-r^2/4R^2) J_0(kr\rho/F)}{(1 + 24\langle a_4^2 \rangle \, r^2/R^2)} . \qquad (67)$$

To make analytical calculations, let us proceed from the intensity distribution $\langle I \rangle$ to the corresponding angular spectrum

$$P(\kappa) = \int \int d^2\rho \, \exp(i\kappa\rho) \, \langle I(F, \rho) \rangle . \qquad (68)$$

Thus we obtain for the case of vacuum

$$P_1(\kappa) = \pi R^2 \exp(-\kappa^2 R^2/4\Omega^2) ,$$

and for the case 2

$$P_2(\kappa) = \frac{\pi R^2}{(1 + 24\langle a_4^2 \rangle \, k^2 R^2/\Omega^2)} \exp(-\kappa^2 R^2/4\Omega^2) . \qquad (69)$$

The characteristic scale of change of the vacuum spectrum $P_1(\kappa)$ is determined by the exponential fall off and corresponds to the frequency $2\Omega/R$ which determines the angular dimension of Airy disk. In the case 2 the spectrum is below the vacuum one:

$$\frac{P_2(\mathrm{k})}{P_1(\mathrm{k})} = (1 + 24{<}a_4^2{>}\,\kappa^2\,R^2/\Omega^2)^{-1} \ .$$

At the characteristic frequency $\kappa \sim 2\Omega/R$ this decrease is numerically equal to $(1 + 96{<}a_4^2{>})^{-1}$.

As a result of correction (case 3) we have

$$P_3(\kappa) = \frac{\pi\,R^2}{(1 + 24{<}a_4^2{>}\,\mathrm{k}^2\,R^2/\Omega^2)} \exp\left\{-\frac{\mathrm{k}^2\,R^2}{4\,\Omega^2} - 6\,\frac{<a_4^2>}{\Omega^2}\,b^2\,\mathrm{k}^2\right\} \times$$

$$\times \cosh\left(12\,\frac{<a_4^2>}{\Omega^2}\,b^2\,\mathrm{k}_y\,\mathrm{k}_z\right)\left\{1 + \frac{48{\cdot}24\,{<}a_4^2{>}^2\,\mathrm{k}^2\,b^2/\Omega^4}{(1 + 24{<}a_4^2{>}\,\mathrm{k}^2\,R^2/\Omega^2)} \times\right.$$

$$\times \left(\kappa^2\,R^2\cosh\left(12\,\frac{<a_4^2>}{\Omega^2}\,b^2\,\mathrm{k}_y\,\mathrm{k}_z\right) + 2\,\kappa_y\,\kappa_z\,R^2 \times\right.$$

$$\left.\left.\times \sinh\left(12\,\frac{<a_4^2>}{\Omega^2}\,b^2\,\mathrm{k}_y\,\mathrm{k}_z\right)\right)\right\} , \qquad (70)$$

where $\kappa = (\kappa_y,\ \kappa_z)$ and b is the distance between the centers of subapertures.

As a result the increase of the spectrum due to the correction made is as follows

$$\left.\frac{P_3(\mathrm{k})}{P_2(\mathrm{k})}\right|_{\mathrm{k}\,=\,2\mathrm{X}/R} \simeq \exp\left(-\,24{<}a_4^2{>}\,b^2/R^2\right) \times$$

$$\times \cosh(48{<}a_4^2{>}\,b^2/R^2)\left\{1 + \frac{8\text{ч}24{\cdot}24\,{<}a_4^2{>}^2\,b^2\ /\ R^4}{1 + 96{<}a_4^2{>}} \times\right.$$

$$\left.\times\,[\cosh(48{<}a_4^2{>}\,b^2/R^2) + \sinh(48{<}a_4^2{>}\,b^2/R^2)]\right\} . \qquad (71)$$

The efficiency of an adaptive correction for defocusing can be numerically derived from Eq. (71) for concrete values of $<a_4^2>$, Ω, and b/R. It is interesting to note the anisotropy of the spectrum $P_3(\kappa)$, Eq. (70). The spectrum reaches its maximum at the diagonals ($\kappa_y = \kappa_z$).

It is clear that the effect of spectrum increase along diagonals (what results in narrowing the intensity distribution) because of four–component adaptive corrector should be greater at larger ratio R/r_0. For example, for $R/r_0 = 4$ the increase is 4.64, and for $R/r_0 = 5$ it is 12.6. Thus, the graph of this distribution looks typically like a four–lobe diagram, with the lowest spread caused by residual phase distortions being observed along diagonals.

These results[21] quite well demonstrate efficiency of the considered simple devices for image correction.

15. NUMERICAL SIMULATION OF AN ADAPTIVE GROUND–BASED TELESCOPE (1991)

At present adaptive optical systems find most efficient applications in astronomy.

It is known that atmospheric turbulence limits the telescope resolution to about 1 second of arc, whereas for $\lambda = 0.5\ \mu\mathrm{m}$ the diffraction–limited resolution of the telescope 3.6 m in diameter is 0.03 seconds. In this section we present the results[22] of calculation of the point–spread function for an adaptive telescope with circular aperture 1 m in diameter at the wavelength of 0.55 μm. We consider two kinds of phase correctors: the mode corrector which

compensates for phase front aberrations from tilts to coma and the compound mirror with hexagonally packed elements.

Our program of simulation of the phase distortions of a plane monochromatic wave, caused by atmospheric turbulent inhomogeneities in the refractive index, consists of two parts. The first one generates phase distortions using Fourier transform method. The spatial scale of the distortions is limited by the step from below and by the size of calculational grid from the above. Second part recalculates scales greater than the size of calculational grid into classical aberrations which are considered as Gaussian random variables with zero average and the variances

$$s_n^2 = 8\pi\,(n + 1) \int\limits_0^{\$} \mathrm{d}\kappa\,\kappa\,\Phi(\kappa)\,\frac{J_{n+1}^2(\mathrm{k}\,R)}{(\mathrm{k}\,R)^2}\ , \qquad (72)$$

where n is the radial degree of the corresponding polynomial, R is circle radius, $J_n(x)$ is Bessel function, $\Phi(\kappa) = 0.489\,r_0^{-5/3}{\cdot}\kappa^{-11/3}$ is the spatial spectrum of phase distortions, and r_0 is Fried's coherence radius.

Hence, our method of simulating turbulent distortions[22] has the following advantages over the known ones: first, the atmospheric coherence length r_0 is the input parameter rather than estimated one; second, our method allows for greater scales than the size of calculational grid; and, third, the random spectral amplitude of distortions is generated in a way to get purely real values of phase distortions.

We present here some results obtained by statistical image averaging. Taking the ensemble–average of random point–spread function, we obtain long–exposure intensity distribution in the image plane $I(\gamma_y,\ \gamma_z)$. Then we calculate energy per circle of radius ω (in Figs. 14–16 radius ω is presented in seconds of arc)

$$E(\omega) = \frac{\displaystyle\iint\limits_{\mathrm{g}_y^2\,+\,\mathrm{g}_z^2\,J\,\mathrm{w}^2} I(\mathrm{g}_y,\ \mathrm{g}_z)\,\mathrm{dg}_y\,\mathrm{dg}_z}{\displaystyle\iint\limits_{-\infty}^{\infty} I(\mathrm{g}_y,\ \mathrm{g}_z)\,\mathrm{dg}_y\,\mathrm{dg}_z}\ ,\quad .$$

Remind that calculations have been performed for the telescope 1 m in diameter and coherence length r_0 of 10 and 20 cm.

Limiting curves in Figs. 14–16 correspond to the diffraction limit and that without correction. For the mode corrector we obtained: curve 1 — correction for common tilt; 2 — correction for common tilt, defocusing, and astigmatism; and, 3 — correction for common tilt, defocusing, astigmatism, and coma. For the compound corrector we performed calculations for a number of segments equal to 7, 19, and 37 with preliminary corrected common tilt at the receiving aperture. Each segment has one, two, or three degrees of freedom that corresponds to correction of either common or local tilt or both of them within the limits of each segment.

We do not present curves corresponding to local tilts correction because this correction does not improve $E(\omega)$ significantly with respect to common tilt correction within the overall aperture. It is seen from figures that correction of local average phase by means of compound mirror gives great increase in the energy per circle of diffractional radius ($\lambda/D \approx 0.1$ second of arc) while the correction of both local average phase and tilt gives $E(\omega)$ close to diffractional distribution for a number of segments 19 and 37. Correction for aberrations starting from tilt to coma inclusive gives also

good results for $r_0 = 20$ cm ($D/r_0 = 5$) but its efficiency reduces fast with increasing turbulence intensity for $r_0 = 10$ cm. The lowest curves in all figures correspond to image forming without any phase correction. It is seen that radius of circle intercepting 80% of energy constitutes 0.55″ for $r_0 = 20$ cm and 1.1″ for $r_0 = 10$ cm what well agrees with the values known from astronomic observations.
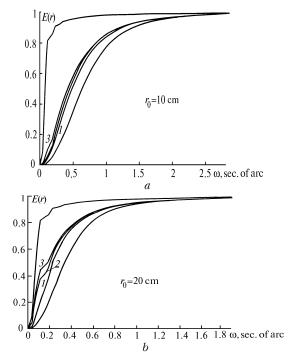

FIG. 14. Efficiency of lowest modes correction: 1) correction for tilt; 2) correction for tilt, defocusing, and astigmatism; and, 3) correction for tilt, defocusing, astigmatism, and coma.
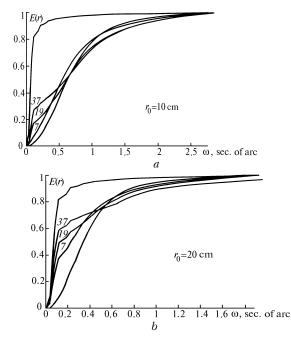

FIG. 15. Efficiency of corrections with a compound mirror: average phase correction for each segment in the cases of 7−, 19−, and 37−component mirror.
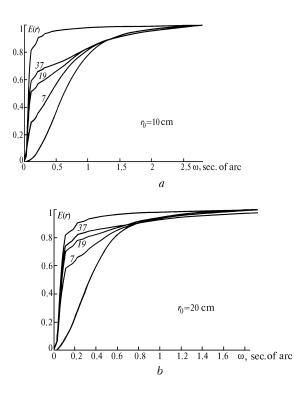

FIG. 16. Correction of the average phase and local tilt for each segment in the cases of 7−, 19−, and 37−component mirror.

16. CALCULATION OF POINT−SPREAD FUNCTION FOR AN ADAPTIVE TELESCOPE WITH HARTMANN WAVE−FRONT SENSOR (1992)

We continue to develop our mathematical model with the successive complications which bring it closer to reality. In this section we present the results[23] of numerical calculation of the point−spread function (PSF) for an adaptive telescope. Our program simulates its main components such as wave−front sensor of Hartmann type and compound corrector representing the array of square−shaped elements.

The intensity distribution in the focal plane of each subaperture was calculated in paraxial approximation, therefore both diffraction and aberrations of the wave front were considered. The photon noise was simulated by means of a Poisson random−number generator.

Below the Hartmann sensor is considered as a device which measures displacements of segments of the wave front of an optical beam focused by the subapertures. The program computes displacements of intensity distribution center in the focal plane of each subaperture with respect to diffractional position and determines with the above−described algorithms the tilts and translations for every component of a corrector. Corrected wave front was used to calculate short−exposure PSF which then was averaged over an ensemble of random turbulent distortions.

During the calculations, simulation of random turbulent distortions of the wave front is being done in the phase screen approximation with the screen placed in the plane of the telescope aperture. Two−dimensional spectral density of the phase fluctuations of a plane wave propagating in the atmosphere in the geometrical−optics approximation is

$$F_S(\kappa) = 0.489\, r_0^{-5/3}\, (\kappa^2 + k_0^2)^{-11/6}\, , \qquad (73)$$

where $r_0 \simeq (0.423\, k^2 \int C_n^2(\xi)\, d\xi)^{-3/5}$ is the Fried's coherence radius, $k = 2\pi/\lambda$ is the wave number, $C_n^2(\xi)$ is the profile of structure constant of the refractive index fluctuations along the propagation path, and $\kappa_0 = 2\pi/L_0$, L_0 is the outer scale of turbulence taken to be 100 m. The inner scale of turbulence does not enter explicitly into the spectrum given by Eq. (73), but in the process of simulation of the turbulent distortions we lose scales being less than a grid pitch and therefore the inner scale appears. It is equal to a grid pitch, which in our experiments is about 2 cm.

We use thus obtained set of random wave front values to compute successively the complex amplitude distribution and the intensity distribution in the focal plane of the collecting lens. The lens aperture function was taken to be unity within a square of 1 m side and zero outside it.

The compound wave–front corrector is an array of square–shaped elements with the side $d = D/N_c^{1/2}$ (where N_c is a number of elements) controlled independently in three different degrees of freedom: tilts along Y and Z axes and translation along X axis. We adopt that corrector and apertures of the wave–front sensor are placed in the planes conjugate with the plane of the telescope aperture.

Wave–front sensor is an array of collecting lenses of the same size and shape as the elements of the corrector array. Distorted image of a monochromatic point source is formed in the focal planes of each subaperture of the sensor. We reconstructed the wave front using measurements of the image intensity distribution.

For this purpose we used mode method of reconstruction of the wave front as the finite sum of Zernike polynomials as well as an original analog method. It should be mentioned here that the analog method does not assume measurements, it is rather a control based on data of phase gradients measurements with Hartmann method.

Performance of this analog method requires construction of a special controllable (active) mirror with the elements whose size and shape must precisely coincide with those of the subaperture of a Hartmann sensor referred to the input pupil of the optical system.

The mirror is a multilayer construction. The first layer supports the whole mirror; the second layer represents an active element which turns the whole mirror surface to an angle corresponding to an average over all subapertures data from the Hartmann sensor. Third layer represents an active element which turns separate segments (there are four segments) to angles corresponding to measured phase gradients averaged over all segments. The next layer is divided into 16 segments more, and so on.

Control of each layer within each element is calculated by simple summation of the measured local phase gradients minus value of the preceding control step.

First of all we present results of PSF calculation obtained assuming that the wave front distortions are known at any point of the aperture. Tilts and translations for each corrector's component are determined by minimizing residual wave front distortions with the least–squares method. These results demonstrate the restrictions connected only with the finite number of a corrector elements.

Figure 17 shows the radial distribution of image intensity obtained by averaging of long–exposure PSF over Y angle. Fig. 17a corresponds to $r_0 = 20$ cm ($D/r_0 = 5$) while Fig. 17b — to $r_0 = 1$ cm ($D/r_0 = 10$). Number of corrector elements N_c was from 1 to 64. In Table V we present values of Strehl ratio St (PSF maximum referred to its diffractional value) and PSF's full width at half maximum (FWHM). The wavelength λ hereinafter equals 0.55 μm.

It is seen that diffraction–limited resolution (FWHM = 0.09″ for $D = 1$ m and $\lambda = 0.55$ μm) is reached just when the size of corrector elements is 3–5 times greater than the coherence length r_0. Further increase of the number of elements only leads to an increase of the intensity.

Below we present the results of PSF calculation for an adaptive telescope using Hartmann–type wave–front sensor and compound wave–front corrector controlled by the algorithm of mode reconstruction of wave front distortions.[23,24]
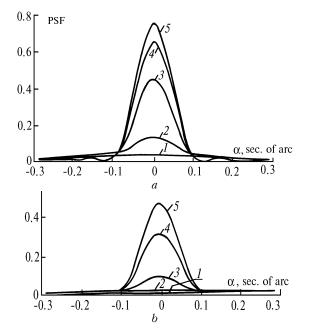

FIG. 17. PSF as a function of angular distance α'' in the case of precise measurements of wave front distortions made using a compound corrector: 1) without correction, 2) $N_c = 1$ (correction of common tilt), 3) $N_c = 4$, 4) $N_c = 16$, and 5) $N_c = 64$; $r_0 = 20$ (a) and $r_0 = 10$ cm (b).

TABLE V.

N_c	d/r_0	St	FWHM
$r_0 = 20$ cm			
—	—	0.03	0.5″
1	5	0.13	0.14″
4	5/2	0.45	0.10″
16	5/4	0.67	0.09″
64	5/8	0.75	0.09″
$r_0 = 10$ cm			
—	—	0.008	1.1″
1	10	0.017	0.64″
4	5	0.089	0.11″
16	5/2	0.31	0.10″
64	5/4	0.46	0.10″

Figures 18a and b show long–exposure PSFs obtained at $r_0 = 20$ cm and $N_s = 16$, with the corresponding values of St and FWHM presented in Table VI. Number of polynomials N_m in mode wave front expansion was taken to be 3, 6, 10, 15, 21, and 28, what corresponds to polynomials of the degree from 1 to 6. The error of wave front reconstruction increases

starting with the number $N_m = 21$. As is seen from Fig. 18 and Table VI, no further increase in the efficiency is observed already at $N_m = 10$. Thus it seems that the number of polynomials equal to the number of the sensor subapertures is quite sufficient when using the algorithm of mode wave front reconstruction.
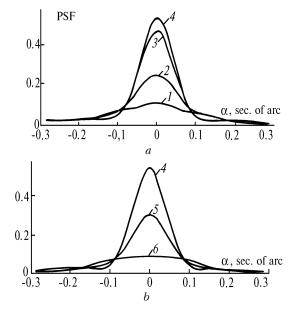

FIG. 18. PSF for the case of mode algorithm of wave front reconstruction for different number of polynomials N_m in the mode expansion (Eq. (66)): 1) $N_m = 3$, 2) $N_m = 6$, 3) $N_m = 10$, 4) $N_m = 15$, 5) $N_m = 21$, and 6) $N_m = 28$; $r_0 = 20$ cm and $N_c = N_s = 16$.

TABLE VI.

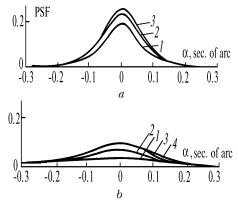| N_m	St	FWHM
3	0.11	0.20″
6	0.25	0.13″
10	0.47	0.10″
15	0.54	0.10″
21	0.30	0.11″
28	0.09	0.27″

FIG. 19. PSF for the case of analog wave front reconstruction: $r_0 = 20$ cm (a)   and $r_0 = 10$ cm (b); 1) $N_s = 4$; 2) $N_s = 16$; 3) $N_s = 64$; and, 4) $N_s = 256$.

For a comparison we present here some results of the PSF calculation by means of analog wave front reconstruction algorithm. The number of subapertures of the wave–front sensors (or that of corrector segments) was taken to be 4, 16, and 64. Results of calculations are presented in Fig. 19 and in Table VII. Although correction here is much worse than in the case of mode wave front reconstruction, we can reach a many times gain in the intensity compared to uncorrected PSF if a sufficient number of sensor subapertures is taken.

TABLE VII.

N_s	d/r_0	St	FWHM
	$r_0 = 20$ cm		
4	5/2	0.2	0.12″
16	5/4	0.24	0.14″
64	5/8	0.26	0.14″
	$r_0 = 10$ cm		
4	5	0.03	0.27″
16	5/2	0.07	0.20″
64	5/4	0.10	0.19″
56	5/8	0.10	0.21″

Finally, we present the results of PSF calculations allowing for a photon noise in the wave–front sensor.[23] Calculations were performed for $r_0 = 20$ cm. In the first case we have varied statistical average of a number of photons N_{ph} at a fixed number of sensor subapertures (see Fig. 20 and Table VIII) while in the second case we have varied the number of subapertures at a fixed number of photons $N_{ph} = 800$ (see Table IX). The number of polynomials in the algorithm of mode wave front reconstruction was taken to be approximately equal to the number of subapertures.
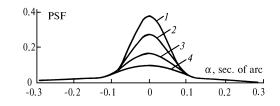

FIG. 20. PSF for the case of mode algorithm allowing for quantum intensity fluctuations: 1) $N_{ph} = 1600$; 2) $N_{ph} = 800$; 3) $N_{ph} = 400$; and, 4) $N_{ph} = 100$; $r_0 = 20$ cm, $N_s = 16$, and $N_m = 15$.

TABLE VIII.

N_{ph}	St	FWHM
1600	0.39	0.11″
800	0.28	0.12″
400	0.17	0.14″
200	0.10	0.20″

TABLE IX.

N_s	N_m	St	FWHM
4	6	0.26	0.12″
16	15	0.28	0.12″
64	28	0.18	0.15″

Therefore, in order to reach the efficiency corresponding to an infinite signal—to—noise ratio one needs about 100 photons for each sensor subaperture (the size of subaperture is approximately equal to the coherence length) during the time when the turbulence is assumed to be frozen.

For a fewer number of photons there exists optimum number of subapertures. If the number of subapertures exceeds this optimum, high level of noise causes strong increase in the error of measuring local tilts of the wave front; in the opposite case the reconstruction error increases due to insufficient spatial resolution of the sensor.[23]

Results of the PSF calculations for an adaptive telescope with Hartmann—type wave—front sensor and a compound corrector, presented in this section, were obtained using the program which can be used by designers of adaptive optical systems in order to choose optimum configuration of wave—front sensors and correctors or to test different algorithms of wave front reconstruction or corrector control.

CONCLUSION

First of all it should be stressed that most of investigations reviewed in this paper do not concern with any specific design of atmospheric optoelectronic systems, e.g., an adaptive telescope. In our investigations we put emphasis to the study of pure atmospheric requirements to adaptive optical systems.[25] Of course, the general direction of such studies has followed some logics and advances reached by the world optical community.

How do we plan further development? First of all, investigations of characteristics of atmospheric optoelectronic systems imply dynamic modelling of all components of an adaptive system as well as of turbulent distortions of the wave front. This should allow us to optimize time of signal storage in the wave—front sensor and to examine different corrector—controlling algorithms, including those that "forecast" future wave front distortions from measurements performed at the present moment.

Our program also implies investigation of the effect of "non—isoplanarity", modelling of artificial reference sources (pseudostars), various types of wave—front sensor (e.g., shear interferometer, Hartmann and wave—front—curvature sensor) and correctors, and also adaptive systems using several wave—front correctors.[25]

Just in 1992 we have performed[24] comparative analysis of the efficiency of deformable and compound mirrors in application to the problem of correcting for turbulent distortions of the wave front.

No doubts that creation of a model of turbulent atmosphere remains of principle importance. Investigations of the potentialities of adaptive systems under the conditions of speckling are also urgent.

ACKNOWLEDGMENTS

REFERENCES

1. V.P. Lukin, Kvant. Elektron. **7**, No. 6, 1270—1279 (1980).
2. A.S. Gurvich, L.I. Kon, et al., *Laser Radiation in the Turbulent Atmosphere* (Nauka, Moscow, 1976), 277 pp.
3. V.P. Lukin, Kvant. Elektron. **8**, No. 10, 2145—2153 (1981).
4. O.N. Emaleev and V.P. Lukin, Kvant. Elektron. **9**, No. 11, 2264—2271 (1982).
5. D. Fried, J. Opt. Soc. Am. **56**, 1372—1379 (1966).
6. V.P. Lukin and M.I. Charnotskii, Kvant. Elektron. **9**, No. 5, 952—958 (1982).
7. S.M. Rytov, Yu.A. Kravtsov, and V.I. Tatarsky, *Introduction to Statistical Radiophysics* (Nauka, Moscow, 1978), Vol. 2, 640 pp.
8. V.P. Lukin and V.V. Pokasov, Kvant. Elektron. **10**, No. 5, 992—1001 (1983).
9. V.P. Lukin and V.F. Matyukhin, Kvant. Elektron. **10**, No. 12, 2465—2473 (1983).
10. V.P. Lukin and V.L. Mironov, Kvant. Elektron. **12**, No. 9, 1959—1962 (1985).
11. V. Lukin and V. Zuev, Appl. Opt. **26**, No. 1, 139—144 (1987).
12. N.N. Botygina, V.P. Lukin, and A.G. Frizen, Kvant. Elektron. **13**, No. 8, 1652—1656 (1986).
13. V.P. Lukin, Kvant. Elektron. **15**, No. 9, 1856—1861 (1988).
14. L.V. Antoshkin, O.N. Emaleev, and V.P. Lukin, Prib. Tekh. Eksp., No. 5, 211—212 (1988).
15. V. Lukin, Opt. Lett. **4**, No. 1, 15—17 (1979).
16. V. Lukin and B. Fortes, Atm. Opt. **4**, No. 12, 905—909 (1991).
17. O.N. Emaleev, V.P. Lukin, et al., in: *Proceedings of the VIII All—Union Symposium on Propagation of Laser Radiation through the Atmosphere* (Tomsk,1986), Vol. 3, pp. 183—185.
18. V.P. Lukin, Opt. Atm. **1**, No. 9, 38—42 (1988).
19. V.P. Lukin, Atm. Opt. **2**, No. 6, 461—468 (1989).
20. L.V. Antoshkin, N.N. Botygina, V.P. Lukin, et al., Atm. Opt. **2**, No. 6, 510—515 (1989).
21. V.P. Lukin, Atm. Opt. **3**, No. 12, 1121—1128 (1990).
22. V.P. Lukin, N.N. Mayer, and B.V. Fortes, Atm. Opt. **4**, No. 12, 1298—1302 (1991).
23. V.P. Lukin, N.N. Mayer, and B.V. Fortes, Atmos. Oceanic Opt. **5**, No. 12, 801—807 (1992).
24. F.Yu. Kanev, V.P. Lukin, and B.V. Fortes, Atmos. Oceanic Opt. **5**, No. 12, 852—854 (1992).
25. V.P. Lukin, *Adaptive Atmospheric Optics* (Nauka, Novosibirsk, 1986), 286 pp.